

Alkynylpyrimidine Amide Derivatives as Potent, Selective, and Orally Active Inhibitors of Tie-2 Kinase

Victor J. Cee,^{*,†,‡} Brian K. Albrecht,^{*,†} Stephanie Geuns-Meyer,[†] Paul Hughes,[§] Steve Bellon,^{||} James Bready,[§] Sean Caenepeel,[§] Stuart C. Chaffee,[†] Angela Coxon,[§] Maurice Emery,[⊥] Jenne Fretland,[⊥] Paul Gallant,[∞] Yan Gu,^{||} Brian L. Hodous,[†] Doug Hoffman,[#] Rebecca E. Johnson,[†] Richard Kendall,[§] Joseph L. Kim,^{||} Alexander M. Long,^{||} David McGowan,[†] Michael Morrison,[∞] Philip R. Olivieri,[†] Vinod F. Patel,[†] Anthony Polverino,[§] David Powers,[∞] Paul Rose,^{||} Ling Wang,[§] and Huilin Zhao^{||}

Departments of Medicinal Chemistry, Molecular Pharmacology, and Molecular Structure, Amgen Inc., One Kendall Square, Bldg. 1000, Cambridge, Massachusetts 02139; Departments of Molecular Pharmacology, Oncology Research, Pharmaceuticals, and Pharmacokinetics and Drug Metabolism, Amgen, Inc., One Amgen Center Drive, Thousand Oaks, California 91320

Received September 25, 2006

The recognition that aberrant angiogenesis contributes to the pathology of inflammatory diseases, cancer, and myocardial ischemia has generated considerable interest in the molecular mechanisms that regulate blood vessel growth. The receptor tyrosine kinase Tie-2 is expressed primarily by vascular endothelial cells and is critical for embryonic vasculogenesis. Interference with the Tie-2 pathway by diverse blocking agents such as soluble Tie-2 receptors, anti-Tie-2 intrabodies, anti-Ang-2 antibodies, and peptide-Fc conjugates has been shown to suppress tumor growth in xenograft studies. An alternative strategy for interfering with the Tie-2 signaling pathway involves direct inhibition of the kinase functions of the Tie-2 receptor. Herein we describe the development of alkynylpyrimidine amide derivatives as potent, selective, and orally available ATP-competitive inhibitors of Tie-2 autophosphorylation.

Introduction

Angiogenesis, the formation of new blood vessels from preexisting vasculature, is essential for embryonic development as well as normal physiological processes such as wound healing and the menstrual cycle.¹ The recognition that aberrant angiogenesis contributes to the pathology of inflammatory diseases,² cancer,³ and myocardial ischemia⁴ has generated considerable interest in the molecular mechanisms that regulate blood vessel growth.⁵ Receptor tyrosine kinases expressed primarily by vascular endothelial cells have emerged as important mediators of angiogenesis.⁶ It has been well-established that activation of KDR (VEGFR2) by vascular endothelial growth factor (VEGF) strongly promotes angiogenesis by enhancing endothelial cell proliferation and survival.⁷ While critical for embryonic vasculogenesis, the determination of the precise role of the Tie-2 receptor (tyrosine kinase with immunoglobulin and epidermal growth factor homology domains-2) in pathological angiogenesis has been complicated by the presence of numerous endogenous ligands, including angiopoietin-1 (Ang-1) and angiopoietin-2 (Ang-2).⁸ While Ang-1 is known to activate Tie-2 by inducing Tie-2 phosphorylation,⁹ Ang-2 has been shown to antagonize the effects of Ang-1,¹⁰ although in some contexts Ang-2 has been observed to induce Tie-2 phosphorylation.^{10,11} Interference with the Tie-2 pathway by diverse blocking agents such as soluble Tie-2 receptors,¹² anti-Tie-2 intrabodies,¹³ and anti-Ang-2 antibodies and peptide-Fc conjugates¹⁴ has been shown

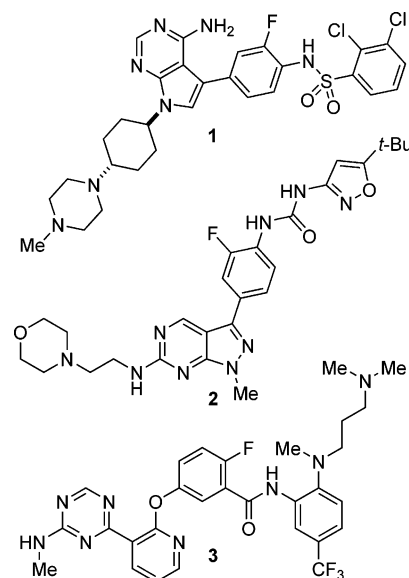


Figure 1. Reported Tie-2 inhibitors.

to suppress tumor growth in xenograft studies. An alternative strategy for interfering with the Tie-2 signaling pathway involves direct inhibition of the kinase functions of the Tie-2 receptor. To this end, we wished to develop an ATP-competitive small molecule inhibitor of Tie-2. In order to establish the effect of Tie-2 kinase inhibition on pathological angiogenesis, it was critical that the small molecule possess selectivity against kinases known to be involved in angiogenesis, particularly KDR.

In contrast to the many reports of small molecule inhibitors of KDR with selectivity against Tie-2,¹⁵ there have been few reports of Tie-2 inhibitors with selectivity against KDR. In 2001, Abbott Laboratories reported the 5-arylpyrrolo[2,3-d]pyrimidin-4-amine derivative **1** (Figure 1) as a potent and selective (>100-fold over KDR enzyme) inhibitor of Tie-2.¹⁶ More recently, compound **2**, based on a structurally related 3-arylpyrazolo-

* To whom correspondence should be addressed. V.J.C.: tel, 805-313-5500; fax, 805-480-1337; e-mail, vcee@amgen.com. B.K.A.: tel, 617-444-5166; fax, 617-577-9822; e-mail, brian.albrecht@amgen.com.

[†] Department of Medicinal Chemistry.

[‡] Present address: Department of Medicinal Chemistry, Amgen, Inc., One Amgen Center Drive, Thousand Oaks, CA 91320.

[§] Department of Oncology Research.

^{||} Department of Molecular Structure.

[⊥] Department of Pharmacokinetic and Drug Metabolism.

[∞] Department of Molecular Pharmacology.

[#] Department of Pharmaceuticals.

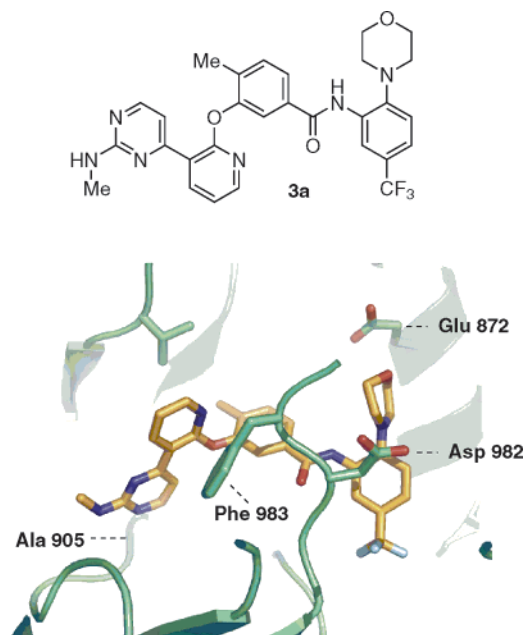


Figure 2. X-ray crystal structure of **3a** bound in the ATP binding site of Tie-2 kinase.

[3,4-*d*]pyrimidine-6-amine core, was reported by GlaxoSmith-Kline as a potent and selective (>140-fold over KDR enzyme) Tie-2 inhibitor.¹⁷ The *in vivo* antiangiogenic activity of both **1** and **2** was demonstrated in murine models of angiogenesis. We recently disclosed the pyridyltriazine amide derivative **3** as a potent ($IC_{50} = 29$ nM) and selective (270-fold over KDR enzyme) inhibitor of Tie-2 with oral bioavailability in rats.¹⁸ Key to the development of **3** was the finding that a 2,5-disubstituted anilide moiety is critical for achieving selectivity over KDR and other kinases. While **3** is an acceptable molecule for the *in vivo* study of Tie-2 inhibition, we recognized that considerable improvements could be made by excising nonessential elements of this molecule. Here we describe the development of alkynylpyrimidine amide derivatives as potent, selective, and orally available Tie-2 inhibitors.

Structural information from cocrystal structures of molecules analogous to **3** (**3a**, Figure 2) and the kinase domain of Tie-2¹⁸ indicated that these molecules bind the inactive “DFG-out” conformation of the protein.^{19,20} The methylaminopyrimidine ring binds to the linker residue Ala905 via two hydrogen bonds, with distances of 3.0 Å (MeNH) and 2.8 Å (N). The aryl amide moiety directs the terminal CF₃-substituted aromatic ring into the extended hydrophobic pocket, and the carbonyl oxygen makes a hydrogen bond with the backbone NH of Asp982 (DFG motif). The pyridine ring plays an important structural role in positioning the pyrimidine ring within H-bonding distance to the linker residues and placing the central aryl ring in the first hydrophobic pocket. While the pyridine ring is observed to participate in an edge-to-face π -stacking interaction with Phe983 of the DFG motif, we questioned whether this interaction was necessary for high binding affinity. This question prompted the series of successive modifications illustrated in Figure 3. Beginning with the nonselective but highly potent **4**, replacement of the pyridylpyrimidine ether with a 2-aminoquinazoline resulted in **5**, with comparable potency.²¹ Analogue **5** could be further simplified by replacement of the quinazoline with an acetylene linkage between the pyrimidine and benzamide portions of the molecule to give **6a**. As this compound was an effective inhibitor of Tie-2 and of considerably reduced molecular weight, an effort to explore the SAR of **6a** was initiated

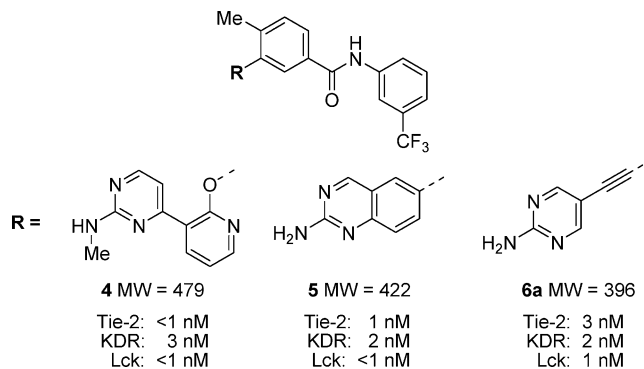


Figure 3. Development of the alkynylpyrimidine amide series.

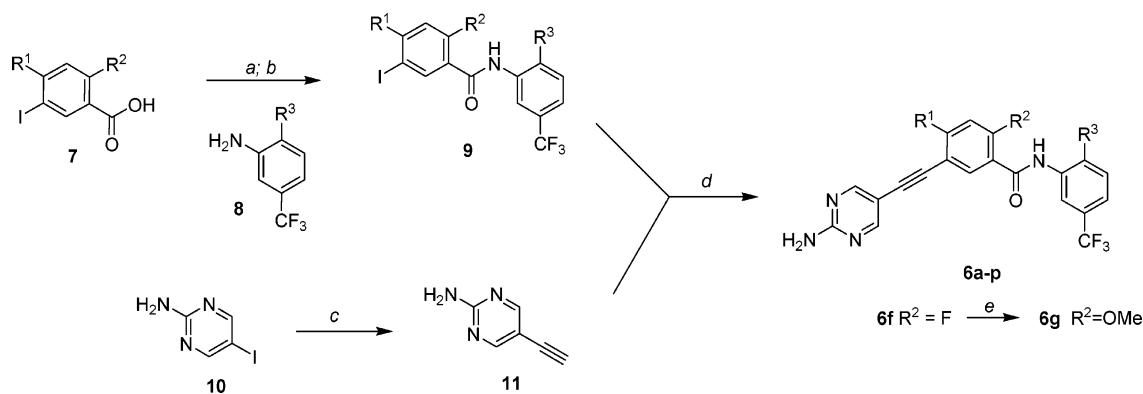
with the goal of improving selectivity while maintaining the impressive potency against Tie-2 kinase.

Chemistry

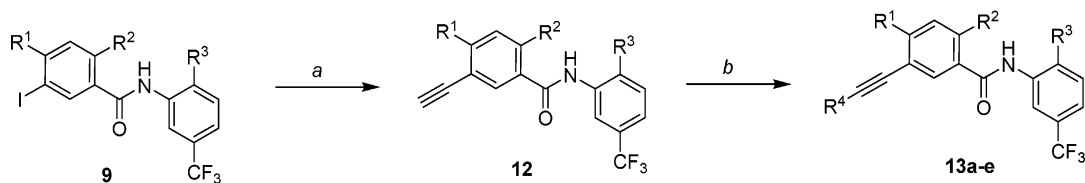
The mild and versatile Sonogashira reaction²² was useful in the synthesis of this class of kinase inhibitor. In an effort to quickly develop SAR, two synthetic schemes were employed. Conversion of benzoic acid derivatives **7** to the corresponding acid chloride followed by amide bond formation with a variety of anilines **8** afforded amides **9** (Scheme 1). Commercially available 5-iodo-2-aminopyrimidine **10** was treated with TMS-acetylene under Sonogashira conditions followed by cleavage of the terminal silane, yielding alkynylpyrimidine **11**. A final Sonogashira coupling of alkynylpyrimidine **11** and aryl iodide **9** produced the requisite core structure **6**. The conversion of aryl fluoride **6f** to **6g** under methanolysis conditions provided additional diversity. In conjunction with the chemistry developed in Scheme 1, it was also feasible to install a variety of heterocycles as the final step (Scheme 2). Aryl iodide **9** was converted to the corresponding terminal acetylene **12** by utilizing conditions similar to those described in Scheme 1. With the acetylene in hand a variety of heteroaromatic halides (R⁴X) were coupled to yield the desired analogues **13**.

The majority of our efforts to afford a kinase inhibitor with the desired profile was focused on modifying the arylbenzamide portion. While some of the requisite anilines are commercially available, the majority were synthesized. Treatment of 4-fluoro-3-nitrobenzotrifluoride **14** with a variety of commercially available amines [piperidine, *N*¹,*N*¹,*N*³,*N*³-tetramethylpropane-1,3-diamine, 4-methylpiperazine, and (*R*)/(*S*)-3-dimethylaminopyrrolidine] and base in THF at elevated temperatures afforded substituted nitroanilines **15** (Scheme 3). Reduction of the nitro group to the corresponding aniline under catalytic hydrogenation conditions provided aniline **8** for coupling in Scheme 1.

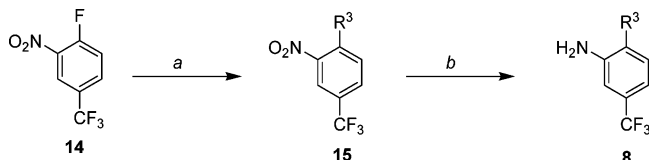
The synthesis of piperidine-substituted anilines for analogues **6j–l** required additional functionalization (Scheme 4). Aniline **8j**, containing a 4-*N,N*-dimethylamino substituent, was prepared from commercially available 1-benzylpiperidin-4-amine, which upon reductive amination, hydrogenolysis, and *N*-arylation with 4-fluoro-3-nitrobenzotrifluoride **14** gave **15j**. Reduction of the nitro group under standard conditions delivered the corresponding aniline **8j**. Enantiomeric anilines **8k** and **8l** containing a 3-*N,N*-dimethylamino-substituted piperidine were prepared separately starting from commercially available (*R*)- and (*S*)-*tert*-butyl piperidin-3-ylcarbamate. Arylation with **14** gave **15k** and **15l**. Removal of the Boc-carbamate with HCl followed by reductive amination with formaldehyde resulted in the corresponding tertiary amines, which were subsequently reduced by hydrogenation to afford anilines **8k** and **8l**.

Scheme 1. General Method A^a

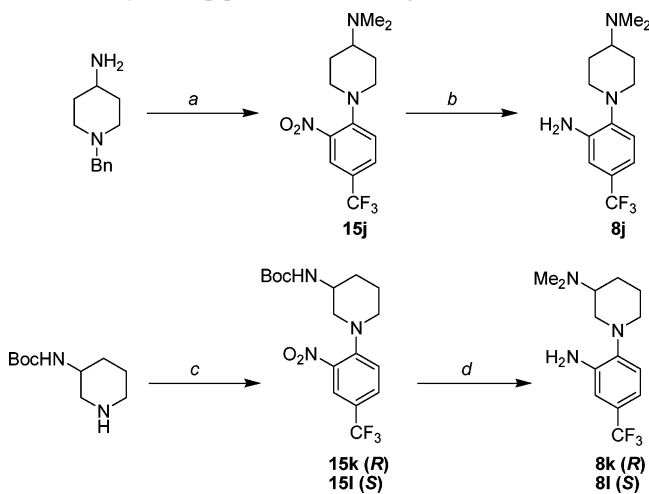
^a Reagents and conditions: (a) SOCl₂, Δ; (b) ^tPr₂NEt, CH₂Cl₂; (c) (i) PdCl₂(PPh₃)₂, CuI, TMS-acetylene, Et₃N, MeCN; (ii) MeOH, K₂CO₃; (d) PdCl₂(PPh₃)₂, CuI, Et₃N, MeCN, Δ; (e) NaOMe, MeOH, Δ.

Scheme 2. General Method B^a

^a Reagents and conditions: (a) PdCl₂(PPh₃)₂, TMS-acetylene, Et₃N, CuI, MeCN, Δ; (b) R⁴X (Br, I) PdCl₂(PPh₃)₂, CuI, Et₃N, MeCN, Δ.

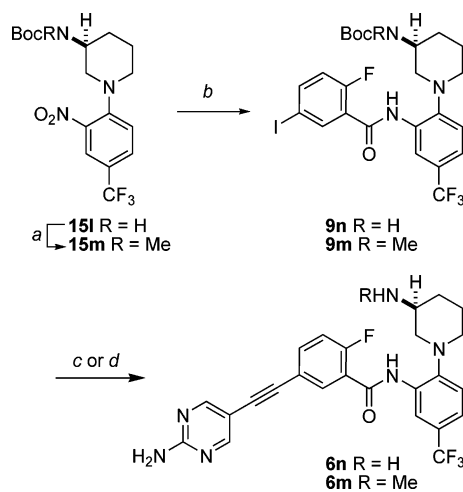
Scheme 3. General Method C^a

^a Reagents and conditions: (a) RR'NH, NaHCO₃, THF, Δ; (b) Pd/C, H₂, MeOH.

Scheme 4. Synthesis of N,N-Dimethylaminopiperidine-Containing Anilines^a

^a Reagents and conditions: (a) (i) HCHO, NaBH₃CN, AcOH/MeOH; (ii) HCl/dioxane/Et₂O; (iii) Pd/C, H₂, MeOH; (iv) 14, TEA, THF, Δ; (b) Pd/C, H₂, MeOH; (c) 14, NaHCO₃, THF, Δ; (d) (i) 4 M HCl in dioxane; (ii) HCHO, NaBH₃CN, HOAc, MeOH; (iii) Pd/C, H₂, MeOH.

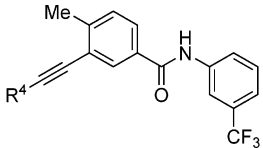
Routes to demethylated analogues **6m/n** were useful in order to produce these potential metabolites of **6l**. Aniline **15l** (Scheme 5) was alkylated with methyl iodide to give **15m** (Scheme 5). Both **15l** and **15m** were processed by a similar sequence according to Scheme 5 to give potential metabolites **6m/n**.

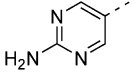
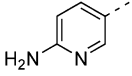
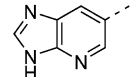
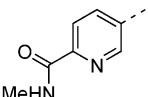
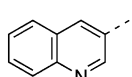
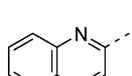
Scheme 5. Synthesis of Demethylated 3-Aminopiperidine Analogues^a

^a Reagents and conditions: (a) NaH, MeI, DMF; (b) (i) Pd/C, H₂, MeOH; (ii) 2-fluoro-5-iodobenzoyl chloride, TEA, CH₂Cl₂. (c) for **9n**, (i) 4 M HCl in dioxane; (ii) **11**, PdCl₂(PPh₃)₂, CuI, Et₃N, MeCN, Δ. (d) for **9m**, (i) **11**, PdCl₂(PPh₃)₂, CuI, Et₃N, MeCN, Δ; (ii) TFA, CH₂Cl₂.

Discussion

The 2-aminopyrimidine moiety of **6a** was envisioned to interact with the linker region of Tie-2 in the ATP-binding cleft via hydrogen bonds between the C=O and N-H of Ala905 and the 2-NH₂ and N of the aminopyrimidine, respectively. The 2-aminopyrimidine could be replaced with other heterocycles containing a similar donor-acceptor motif with no discernible change in inhibitory potency (Table 1, **13a,b**). Although the picolinamide moiety has been employed successfully in other kinase inhibitors,²³ in the case of **13c**, this proved to be an inferior linker-binding element for Tie-2. Quinoline (**13d**) and quinoxaline (**13e**) heterocycles were tolerated, but these molecules were less potent than **6a**. We concluded that modification of the linker-binding element offered little in the way of

Table 1. SAR of Heterocyclic Alkynyl Amide Derivatives^a


Compound	R ⁴	IC ₅₀ (nM)		
		Tie-2	KDR	LcK
6a		3	2	1
13a		3	1	1
13b		2	<1	<1
13c		623	169	154
13d		10	1	1
13e		85	4	4

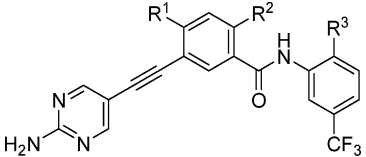
^a Final [ATP]: 5.0 μ M (Tie-2), 1.0 μ M (KDR), 0.5 μ M (Lck).

selectivity, and that the 2-aminopyrimidine was suitable for further SAR studies.

Given the similarity of the *N*-arylbenzamide portion of **6a** and **3** (Figure 1), modification of this region of the molecule was expected to be an effective means of achieving selectivity against KDR.¹⁸ While substitution of the benzamide ring did not provide useful kinase selectivity, para (R¹) and ortho (R²) substitution was found to be important in conjunction with substitution of the *N*-aryl group (R³), as illustrated in Table 2. The desmethyl analogue **6b** exhibited reduced potency relative to **6a**, presumably due to loss of favorable hydrophobic interactions. An *o*-fluoro substituent (**6c**) resulted in a further degradation of Tie-2 inhibitory activity. In this series of compounds, the fluorine-substituted benzamide **6c** is the least

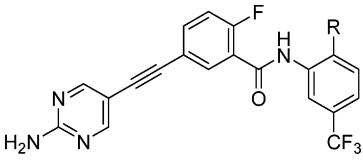
potent of **6a–c**. Incorporation of a bulky, hydrophobic substituent such as piperidine at R³ provided selectivity over KDR (**6d–f**), as anticipated on the basis of the SAR of **3** (Figure 1). Surprisingly, in this series of compounds, the fluorine-substituted benzamide **6f** is the most potent of **6d–f**. This trend was also reflected in an Ang-1-stimulated Tie-2 phosphorylation assay in the EA.hy 926 endothelial cell line. Apparently, the presence of the *o*-fluorine is beneficial only in conjunction with a bulky *N*-aryl group (R³). As the bulky *N*-aryl group (R³) prevents a hydrogen-bonding interaction between the amide N–H and Glu872 of Tie-2 (Figure 2),¹⁸ we speculated that the fluorine substituent provides a favorable electrostatic interaction²⁴ with the free amide N–H, reducing the desolvation penalty upon binding to Tie-2. The plausibility of this theory was tested with **6g**, which contains an *o*-methoxy substituent to serve as a hydrogen-bond acceptor for the amide N–H. Indeed, this compound has approximately the same inhibitory activity as **6f**, which supports the hypothesis that engagement of the amide N–H results in more potent Tie-2 inhibitors. Moreover, selectivity vs KDR and Lck was maintained; however, the compound exhibited reduced cellular activity, which may be due to poor permeability. The optimal molecule in the series **6a–g** was **6f**, due to its potency (Tie-2 IC₅₀ = 17 nM) and selectivity (28-fold over KDR, 21-fold over Lck). **6f** was further shown to inhibit Ang-1-stimulated Tie-2 autophosphorylation in the Ea.hy 926 endothelial cell line with an IC₅₀ of 22 nM.

Despite the favorable in vitro activity of compound **6f**, it was found to be a poor candidate for in vivo studies due to minimal aqueous solubility (<1 μ g/mL, 0.01 N HCl). Our attention focused on the incorporation of anilides containing basic amines to improve the physical properties of this series (Table 3). Incorporation of a tetramethylpropane-1,3-diamine moiety, which had previously provided a high level of selectivity in a related series (**3**, Figure 1), resulted in a relatively nonselective compound (**6h**). It was hypothesized that the lack of selectivity was due to the conformational flexibility of the tetramethylpropane-1,3-diamine substituent; therefore, more rigid ortho-substituents were explored (**6i–p**). A 4-*N*-methylpiperazine substituent (**6i**) proved to be an effective means of incorporating a basic amine while selectivity (84-fold over KDR, 16-fold over Lck) was maintained, although the cellular activity of the compound was somewhat lower than expected. Substitution of *N,N*-dimethylamines onto a piperidine framework was also explored, with 4-substitution (**6j**) being markedly inferior to 3-substitution (**6k/l**). The (*S*) stereochemistry was found to be

Table 2. SAR of the *N*-Arylbenzamide Portion of Pyrimidine Alkynyl Amides^a


compd	R ¹	R ²	R ³	IC ₅₀ (nM)			inhibn of cellular Tie-2 phosphorylation (EA.hy 926)
				enzyme			
				Tie-2	KDR	Lck	
6a	Me	H	H	3	2	1	NT
6b	H	H	H	11	<1	19	NT
6c	H	F	H	47	6	65	NT
6d	Me	H	piperidine	30	>1000	42	39
6e	H	H	piperidine	63	>1000	410	250
6f	H	F	piperidine	17	480	370	22
6g	H	OMe	piperidine	21	390	>25000	1200

^a Final [ATP]: 5.0 μ M (Tie-2); 1.0 μ M (KDR); 0.5 μ M (Lck).

Table 3. SAR of the *N*-Arylbenzamide Portion of Pyrimidine Alkynyl Amides^a


compd	R	IC ₅₀ (nM)			inhibn of cellular Tie-2 phosphorylation (EA.hy 926)
		enzyme			
		Tie-2	KDR	Lck	
6f	piperidine	17	480	370	22
6h	<i>N</i> ¹ , <i>N</i> ¹ , <i>N</i> ³ , <i>N</i> ³ -tetramethylpropane-1,3-diamine	8	11	21	NT
6i	4-methylpiperazine	13	1100	210	84
6j	4-dimethylaminopiperidine	620	170	150	NT
6k	(<i>R</i>)-3-dimethylaminopiperidine	44	810	780	98
6l	(<i>S</i>)-3-dimethylaminopiperidine	5	1030	130	8
6m	(<i>S</i>)-3-methylaminopiperidine	14	1010	620	26
6n	(<i>S</i>)-3-aminopiperidine	13	800	1480	33
6o	(<i>R</i>)-3-dimethylaminopyrrolidine	220	890	1920	NT
6p	(<i>S</i>)-3-dimethylaminopyrrolidine	140	3000	1100	NT

^a Final [ATP]: 5.0 μM (Tie-2); 1.0 μM (KDR); 0.5 μM (Lck).

Table 4. Kinase Selectivity of **6l**

enzyme IC ₅₀ (nM)		
<i>PTK Group I</i> Fgr = 43 Lck = 130 Lyn = 180	<i>PTK Group VII</i> Jak1 = 1,300 Jak2 = 550 Jak3 = 1,700	<i>PTK Group XVI</i> INSR = 2,900 <i>PTK Group XIX</i> TrkA = 18
<i>PTK Group II</i> Itk = >5,000	<i>PTK Group XI</i> EphB4 = 290	<i>PTK Group XXI</i> cMet = >6700
<i>PTK Group III</i> CSK = 1,800	<i>PTK Group XIII</i> Tie-2 = 5	<i>CMGC Group I</i> cdk5 = >100,000
<i>PTK Group IV</i> Fes = 910	<i>PTK Group XIV</i> KDR = 1,000 c-Kit = 2,800 PDGFR = >5,000	<i>CMGC Group II</i> p38α = >8300

ideal, with compound **6l** exhibiting potent inhibition of the Tie-2 kinase domain (IC₅₀ = 5 nM) and Ang-1-stimulated Tie-2 phosphorylation in endothelial cells (IC₅₀ = 8 nM) along with high selectivity (205-fold over KDR, 25-fold over Lck). In addition, the aqueous solubility of **6l** (>200 μg/mL, 0.01 N HCl) was considerably improved over that of **6f** (<1 μg/mL, 0.01 N HCl). We recognized the potential for the dealkylative metabolism of **6l**, and the sequentially demethylated analogues **6m** and **6n** were prepared and found to be potent and selective Tie-2 inhibitors. Finally, we established that *N,N*-dimethylamino-substituted pyrrolidines (**6o,p**) were inferior to *N,N*-dimethylamino-substituted piperidines (**6k,l**).

Compound **6l** was screened against a panel of tyrosine and serine/threonine kinases (Table 4) and was found to be >20-fold selective over many kinases, with the exception of the nerve growth factor receptor kinase TrkA²⁵ (4-fold) and Src family member FGR²⁶ (9-fold). Importantly, **6l** was selective against kinases known to be involved in angiogenesis (58-fold over EphB4, 205-fold over KDR, and >1000-fold over PDGFR). The selectivity profile of **6m** and **6n** was found to be very similar to that of **6l**.

The *in vitro* and *in vivo* pharmacokinetic properties of compounds **6l–n** are summarized in Table 5. Compound **6l**, bearing the *N,N*-dimethylamino substituent, exhibited relatively high clearance (2.4 L/h/kg) when dosed intravenously in male rats. It was speculated that facile *N*-demethylation contributed to the high clearance of **6l**, and the low clearance exhibited by sequentially demethylated compounds **6m** and **6n** is consistent with this hypothesis. Additional evidence in support of this

hypothesis was provided by *in vitro* incubations of **6l** and rat liver microsomes (RLM). **6l** exhibited high clearance (677 μL/min/mg), and compounds **6m** and **6n** were produced.²⁷ In contrast to the high clearance exhibited in rat liver microsomes, compound **6l** was cleared at a much slower rate (<50 μL/min/mg) in mouse liver microsomes (MLM). Compounds **6m** and **6n** were much more consistent across these species with respect to liver microsomal clearance. The mouse microsomal clearance data suggested that all three compounds **6l–n** were good candidates for our mouse-based pharmacodynamic assay (*vide infra*). It was also shown that **6l–n** could be dosed orally in rats with acceptable bioavailability (*F* = 39–54%), supporting *po* administration. Compounds **6l** and **6m** were ultimately chosen for further *in vivo* studies.

The ability of **6l** to modulate Tie-2 phosphorylation levels *in vivo* was assessed in a mouse pharmacodynamic model (Figure 4). A single dose of compound was administered to female CD-1 NU/NU mice *po* at 10, 30, and 100 mg/kg at time zero. Human angiotensin-1 (h-Ang-1) was administered *iv* after 2.75 h to stimulate Tie-2 phosphorylation. Mouse lungs were harvested at 3 h and phosphorylated Tie-2 levels were measured by Western blot analysis. A dose-dependent inhibition of stimulated Tie-2 phosphorylation was observed, with Tie-2 phosphorylation reduced to sub-basal levels at the 30 and 100 mg/kg doses. The 10 mg/kg dose provided an approximately 50% reduction in stimulated Tie-2 phosphorylation, with a plasma concentration of **6l** at 1660 nM. This concentration is 208-fold greater than the cellular IC₅₀ of **6l** (8 nM). However, taking into account nonspecific binding to mouse plasma proteins (**6l** = 97.9% bound in mouse plasma), the free unbound fraction of **6l** is 32 nM and this correlates fairly well with the IC₅₀ determined in the cell-based assay (8 nM). Monomethyl derivative **6m** produced a qualitatively similar result. The robust inhibition of Tie-2 phosphorylation upon *po* administration of **6l** and **6m** indicates that these molecules are suitable for the *in vivo* study of Tie-2 signaling in angiogenesis.

Conclusions

An effort to reduce the molecular weight of pyridyl-triazine Tie-2 inhibitor **3** by excising less important elements of the molecule led to a series of alkynylpyrimidine amide derivatives. Modification of the *N*-arylbenzamide portion of these molecules provided selectivity over other kinases. The combination of an

Table 5. Pharmacokinetic Properties of **6l–n**

compd	R	Cl ($\mu\text{L}/\text{min}/\text{mg}$)		Cl ^b (L/h/kg)	V _{ss} ^b (L/kg)	T _{1/2} ^b (h)	AUC _{0–∞} ^c (ng h/mL)	F ^c (%)
		RLM	MLM					
6l	NMe ₂	677	<50	2.4	11.8	7.9	800	39
6m	NHMe	<50	<50	0.15	2.2	10.6	18,600	54
6n	NH ₂	<100	<100	0.32	4.6	11.4	9,300	51

^a Male Sprague–Dawley rats ($n = 3$). ^b iv, 2.0 mg/kg. (DMSO). ^c po, 5.0 mg/kg (pH 2.2 OraPlus).

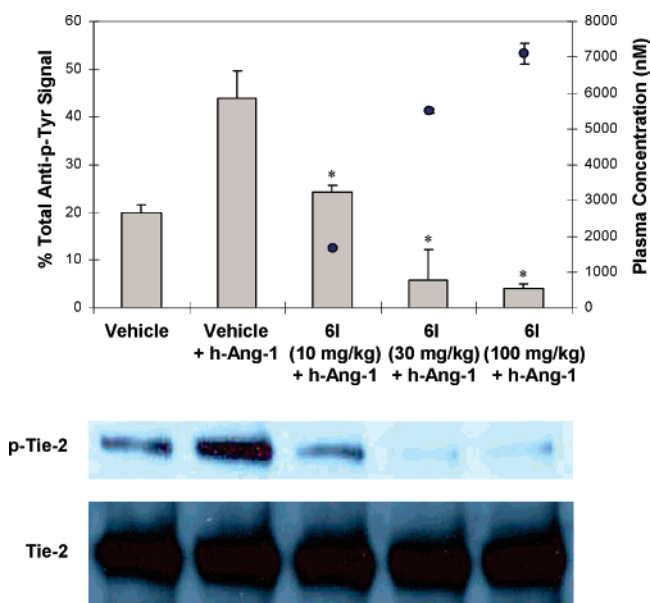


Figure 4. Compound **6l** inhibits h-Ang-1-stimulated Tie-2 phosphorylation in mouse lungs. Data points represent the mean \pm SE, $n = 3$; (*) $p \leq 0.05$ vs vehicle + h-Ang-1 by one-way ANOVA with Dunnett's posthoc test. Bars and p-Tie-2 represent phosphorylated Tie-2, and circles represent plasma concentration.

o-fluorine substituent on the aryl carboxamide with an *o*-piperidine substituent on the aniline fragment was found to be ideal in terms of potency and selectivity. Installation of basic amines onto the piperidine framework provided compounds with greatly improved physical properties. Compounds **6l** and **6m** exhibited favorable pharmacokinetic properties in rat and are suitable for oral dosing ($F = 39$ and 54% , respectively). In a mouse pharmacodynamic model, **6l** exhibited a dose-dependent inhibition of Ang-1-stimulated Tie-2 phosphorylation in lung tissue, with suppression of Tie-2 phosphorylation below basal levels after a single dose of 30 mg/kg (po). Monomethyl derivative **6m** produced a qualitatively similar result. These data indicate that **6l** and **6m** are suitable small molecules for the *in vivo* study of Tie-2 signaling in angiogenesis.

Experimental Section

Unless otherwise noted, all materials were obtained from commercial suppliers and used without further purification. Anhydrous solvents were obtained from Aldrich and used directly. All reactions involving air- or moisture-sensitive reagents were performed under a nitrogen or argon atmosphere. Silica gel

chromatography was performed using either glass columns packed with silica gel (200–400 mesh, Aldrich Chemical) or medium-pressure liquid chromatography (MPLC) on a CombiFlash Companion (Teledyne Isco) with RediSep normal-phase silica gel (35–60 μm) columns and UV detection at 254 nm. Preparative reversed-phase HPLC was performed on a Gilson (215 liquid handler), YMC-Pack Pro C18, 150 \times 30 mm i.d. column, eluting with a binary solvent system using a gradient elution (A, H₂O with 0.1% TFA; B, CH₃CN with 0.1% TFA) with UV detection at 254 nm. All final compounds were purified to >95% purity as determined by high performance liquid chromatography (HPLC) with an Agilent 1100 Series instrument and UV detection at 254 nm (system A, Zorbax SB-C8, 4.6 \times 150 mm, 15 min, 1.5 mL/min flow rate, from 5 to 95% 0.1% TFA in CH₃CN/from 95 to 5% 0.1% TFA in H₂O; system B, Phenomenex Synergi, 2 \times 50 mm, 3 min, 1.0 mL/min flow rate, from 5 to 95% 0.1% formic acid in CH₃CN/from 95 to 5% 0.1% formic acid in H₂O; system C, Zorbax SB-C8, 4.6 \times 75 mm, 12 min, 1.0 mL/min flow rate, from 10 to 90% 0.1% formic acid in CH₃CN/from 90 to 10% 0.1% formic acid in H₂O). NMR spectra were determined with either a Bruker AV-400 (400 MHz) spectrometer or a Varian 400 or 300 MHz spectrometer at ambient temperature. Low-resolution mass spectral (MS) data were determined on an Agilent 1100 Series LC–MS with UV detection at 254 nm and a low resonance electrospray mode (ESI). Chemical shifts are reported in ppm from the solvent resonance (DMSO-*d*₆, 2.50 ppm). Data are reported as follows: chemical shift, multiplicity (s = singlet, d = doublet, t = triplet, q = quartet, br = broad, m = multiplet), coupling constants, and number of protons. High-resolution mass spectra (HRMS) were obtained on a high resolution electrospray time-of-flight mass spectrometer (Agilent). Combustion analysis was performed by Galbraith Laboratories, Inc., Knoxville, TN.

General Method A. 3-Halobenzoic acid **7** (10 mmol) was taken up in SOCl₂ (4 mL). The resulting slurry was heated to reflux for 2 h, at which time the reaction was cooled and concentrated under reduced pressure to afford the corresponding acid chloride, which was used without further purification.

The acid chloride (1 equiv) was taken up in CH₂Cl₂ (0.1 M) followed by the addition of ^tPr₂NEt (1.2 equiv) and the appropriate aniline **8** (1 equiv). The mixture was allowed to stir at room temperature for 3 h. The reaction mixture was diluted with CH₂Cl₂ and washed with water, saturated aqueous NaHCO₃, and brine. The organic layer was dried over anhydrous sodium sulfate, filtered, and concentrated under reduced pressure to afford benzamide **9**, which was used without further purification.

5-Ethynylpyrimidin-2-amine **11** (2 equiv), benzamide **9** (1 equiv), and PdCl₂(PPh₃)₂ (0.05 equiv) were taken up in MeCN:Et₃N (3:1, 0.1 M) in a sealable tube. To the resulting mixture was added CuI (0.05 equiv) and the reaction vessel was sealed and heated to 80 °C until complete consumption of benzamide **9** was observed by LC–MS analysis (typically 2h). The reaction mixture was

concentrated under reduced pressure and purified by silica gel chromatography or reverse-phase HPLC to afford the title compounds.

General Method B. Benzamide **9** (1 equiv) and PdCl₂(PPh₃)₂ (0.05 equiv) were taken up in MeCN:Et₃N (3:1, 0.1 M) followed by the addition of TMS-acetylene (5 equiv) and CuI (0.05 equiv). The reaction mixture was allowed to stir at ambient temperature until complete consumption of the benzamide was observed. To this mixture was added excess K₂CO₃ and the mixture was allowed to stir for approximately 1.5 h. The mixture was filtered through a pad of Celite. To the filtrate was added silica gel, and the mixture was concentrated under reduced pressure and purified via automated flash chromatography (silica gel, from 10% to 50% EtOAc in hexanes, gradient elution) to afford the desired terminal acetylene **12**.

To a solution of heteroaromatic halide (2 equiv), alkyne **12** (1 equiv), and PdCl₂(PPh₃)₂ (1 equiv) in MeCN:Et₃N (3:1, 0.1 M) was added CuI (0.05 equiv). The tube was sealed and heated to 90 °C for 1 h. The mixture was cooled to ambient temperature, concentrated under reduced pressure, and purified either by silica gel chromatography or reverse-phase HPLC to afford title compounds **13**.

General Method C. To a round-bottom flask was added RR'NH (1 equiv), sodium bicarbonate (2.5 equiv), and 1-fluoro-2-nitro-4-(trifluoromethyl)benzene **14** (1 equiv). The mixture was diluted with THF (0.1 M), fitted with a water-cooled reflux condenser, and was heated to 70 °C. After 14 h, the orange mixture was cooled to ambient temperature, and filtered through a glass frit, rinsing with EtOAc. The filtrate was concentrated under reduced pressure and was purified by recrystallization from hexanes or silica gel chromatography. The resulting nitrobenzene was taken up in MeOH (0.1 M), purged with argon, and treated with Pd/C (10%, 0.1 equiv). The flask was fitted with an H₂ balloon and allowed to stir at ambient temperature. Upon completion of the reaction, the vessel was purged with argon, the reaction was filtered through a bed of Celite, and the filtrate was concentrated under reduced pressure to afford title anilines **8**, which were used without further purification.

3-(2-(2-Aminopyrimidin-5-yl)ethynyl)-4-methyl-N-(3-(trifluoromethyl)phenyl)benzamide (6a) was prepared according to general method A starting from 3-iodo-4-methyl-N-(3-(trifluoromethyl)phenyl)benzamide (0.17 g, 0.42 mmol) to give **6a** as an off-white solid (0.046 g, 27%): ¹H NMR (400 MHz, DMSO-*d*₆) δ ppm 10.57 (s, 1 H), 8.48 (s, 2 H), 8.25 (s, 1 H), 8.11 (s, 1 H), 8.08 (d, *J* = 8.1 Hz, 1 H), 7.85–7.93 (m, 1 H), 7.61 (t, *J* = 8.1 Hz, 1 H), 7.50 (d, *J* = 8.1 Hz, 1 H), 7.46 (d, *J* = 7.7 Hz, 1 H), 7.22 (s, 2 H), 2.52 (s, 3 H); HRMS *m/z* = 397.1276 [M + H]⁺, calcd [C₂₁H₁₅F₃N₄O + H]⁺ = 397.1271; HPLC *t*_R A, 8.86 min; C, 7.68 min.

3-(2-(2-Aminopyrimidin-5-yl)ethynyl)-N-(3-(trifluoromethyl)phenyl)benzamide (6b) was prepared according to general method A starting from 3-iodo-N-(3-(trifluoromethyl)phenyl)benzamide (0.10 g, 0.26 mmol) to give **6b** (0.067 g, 69%) as a white solid: ¹H NMR (400 MHz, DMSO-*d*₆) δ ppm 10.64 (s, 1 H), 8.47 (s, 2 H), 8.26 (s, 1 H), 8.13 (s, 1 H), 8.08 (d, *J* = 8.0 Hz, 1 H), 7.97 (d, *J* = 7.8 Hz, 1 H), 7.74 (d, *J* = 8.0 Hz, 1 H), 7.57–7.67 (m, 2 H), 7.48 (d, *J* = 7.5 Hz, 1 H), 7.20 (s, 2 H); HRMS *m/z* = 383.1121 [M + H]⁺, calcd [C₂₀H₁₃F₃N₄O + H]⁺ = 383.1114. Anal. (C₂₀H₁₃F₃N₄O·0.25H₂O) C, H, N.

5-(2-(2-Aminopyrimidin-5-yl)ethynyl)-2-fluoro-N-(3-(trifluoromethyl)phenyl)benzamide (6c) was prepared according to general method A starting from 2-fluoro-5-iodo-N-(3-(trifluoromethyl)phenyl)benzamide (0.30 g, 0.73 mmol) to give **6c** as an off-white solid (0.045 g, 15%): ¹H NMR (400 MHz, acetone-*d*₆) δ ppm 9.81 (s, 1 H), 8.43 (s, 2 H), 8.30 (s, 1 H), 8.04 (d, *J* = 8.4 Hz, 1 H), 7.95 (dd, *J* = 6.6, 2.2 Hz, 1 H), 7.73 (ddd, *J* = 8.4, 4.8, 2.2 Hz, 1 H), 7.63 (t, *J* = 8.1 Hz, 1 H), 7.50 (d, *J* = 7.7 Hz, 1 H), 7.36 (dd, *J* = 10.4, 8.6 Hz, 1 H), 6.49 (s, 2 H); HRMS *m/z* = 401.1030 [M + H]⁺, calcd [C₂₀H₁₂F₄N₄O + H]⁺ = 401.1020. Anal. (C₂₀H₁₂F₄N₄O·H₂O) C, H, N.

3-(2-(2-Aminopyrimidin-5-yl)ethynyl)-4-methyl-N-(2-(piperidin-1-yl)-5-(trifluoromethyl)phenyl)benzamide (6d) was prepared

according to general method A starting from 3-iodo-4-methyl-N-(2-(piperidin-1-yl)-5-(trifluoromethyl)phenyl)benzamide (0.13 g, 0.26 mmol) to give **6d** (0.12 g, 99%): ¹H NMR (400 MHz, DMSO-*d*₆) δ ppm 9.65 (s, 1 H), 8.46 (s, 2 H), 8.30–8.40 (m, 1 H), 7.99–8.14 (m, 1 H), 7.86 (dd, *J* = 8.0, 1.6 Hz, 1 H), 7.46–7.55 (m, 2 H), 7.37 (d, *J* = 8.3 Hz, 1 H), 7.21 (s, 2 H), 2.85–2.94 (m, 4 H), 2.53 (s, 3 H), 1.66–1.76 (m, 4 H), 1.49–1.62 (m, 2 H); HRMS *m/z* = 502.1834 [M + Na]⁺, calcd [C₂₆H₂₄F₃N₅O + Na]⁺ = 502.1825; HPLC *t*_R A, 9.79 min; B, 2.75 min.

3-(2-(2-Aminopyrimidin-5-yl)ethynyl)-N-(2-(piperidin-1-yl)-5-(trifluoromethyl)phenyl)benzamide (6e) was prepared according to general method A starting from 3-iodo-N-(2-(piperidin-1-yl)-5-(trifluoromethyl)phenyl)benzamide (0.13 g, 0.26 mmol) to give **6e** (0.12 g, quant.) as a light yellow solid: ¹H NMR (400 MHz, DMSO-*d*₆) δ ppm 9.72 (s, 1 H), 8.45 (s, 2 H), 8.32 (s, 1 H), 8.07 (s, 1 H), 7.95 (d, *J* = 8.0 Hz, 1 H), 7.74 (d, *J* = 7.7 Hz, 1 H), 7.63 (dd, *J* = 7.7 Hz, 1 H), 7.51 (dd, *J* = 8.5, 1.3 Hz, 1 H), 7.37 (d, *J* = 8.2 Hz, 1 H), 7.21 (s, 2 H), 2.84–3.00 (m, 4 H), 1.64–1.77 (m, 4 H), 1.50–1.61 (m, 2 H); HRMS *m/z* = 488.1674 [M + Na]⁺, calcd [C₂₅H₂₂F₃N₅O + Na]⁺ = 488.1669; HPLC *t*_R A, 9.50 min; B, 2.70 min.

5-(2-(2-Aminopyrimidin-5-yl)ethynyl)-2-fluoro-N-(2-(piperidin-1-yl)-5-(trifluoromethyl)phenyl)benzamide (6f) was prepared according to general method A starting from 2-fluoro-5-iodo-N-(2-(piperidin-1-yl)-5-(trifluoromethyl)phenyl)benzamide (0.20 g, 0.41 mmol) to give **6f** (0.21 g, quant.) as an off-white solid: ¹H NMR (400 MHz, DMSO-*d*₆) δ ppm 9.94 (d, *J* = 9.9 Hz, 1 H), 8.65 (s, 1 H), 8.47 (s, 2 H), 7.78 (m, 1 H), 7.45–7.56 (m, 4 H), 7.22 (s, 2 H), 2.86–2.88 (m, 4 H), 1.71 (m, 4 H), 1.56 (m, 2 H); HRMS *m/z* = 506.1573 [M + Na]⁺, calcd [C₂₅H₂₁F₄N₅O + Na]⁺ = 506.1574; HPLC *t*_R A, 10.35 min; B, 2.79 min.

5-(2-(2-Aminopyrimidin-5-yl)ethynyl)-2-methoxy-N-(2-(piperidin-1-yl)-5-(trifluoromethyl)phenyl)benzamide (6g). A mixture of 5-(2-(2-aminopyrimidin-5-yl)ethynyl)-2-fluoro-N-(2-(piperidin-1-yl)-5-(trifluoromethyl)phenyl)benzamide (0.14 g, 0.29 mmol) and NaOMe (0.5 M solution in methanol, 2.0 mL, 1.0 mmol) in a sealed tube was heated to reflux. After 16 h, the reaction was cooled and partitioned between EtOAc and brine. The organic layer was dried over anhydrous sodium sulfate, filtered, and concentrated. The material was purified by preparative TLC, eluting with 30% acetone/dichloromethane to give **6g** as a white solid (0.037 g, 26%): ¹H NMR (400 MHz, DMSO-*d*₆) δ ppm 10.49 (s, 1 H), 8.72–8.80 (m, 1 H), 8.45 (s, 2 H), 8.17 (d, *J* = 2.1 Hz, 1 H), 7.74 (dd, *J* = 8.7, 2.3 Hz, 1 H), 7.33–7.51 (m, 3 H), 7.15 (s, 2 H), 4.13 (s, 3 H), 2.76–2.95 (m, 4 H), 1.65–1.80 (m, 4 H), 1.53–1.64 (m, 2 H); HRMS *m/z* = 518.1775 [M + Na]⁺, calcd [C₂₆H₂₄F₃N₅O₂ + Na]⁺ = 518.1774. Anal. (C₂₆H₂₄F₃N₅O₂) C, H, N.

5-(2-(2-Aminopyrimidin-5-yl)ethynyl)-N-(2-((3-(dimethylamino)propyl)(methyl)amino)-5-(trifluoromethyl)phenyl)-2-fluorobenzamide (6h) was prepared according to general method A starting from N-(2-((3-(dimethylamino)propyl)(methyl)amino)-5-(trifluoromethyl)phenyl)-2-fluoro-5-iodobenzamide (0.23 g, 0.41 mmol), affording **6h** as an off-white solid (0.20 g, 95%): ¹H NMR (400 MHz, DMSO-*d*₆) ppm 9.96 (d, *J* = 7.7 Hz, 1 H), 8.50 (s, 1 H), 8.46 (s, 2 H), 8.02 (d, *J* = 5.5 Hz, 1 H), 7.70–7.84 (m, 1 H), 7.37–7.59 (m, 3 H), 7.22 (s, 2 H), 2.90–3.09 (m, 2 H), 2.68 (s, 3 H), 2.15 (t, *J* = 7.0 Hz, 2 H), 1.99 (s, 6 H), 1.47–1.65 (m, 2 H); HRMS *m/z* = 515.2186 [M + H]⁺, calcd [C₂₆H₂₆F₄N₆O + H]⁺ = 515.2177. Anal. (C₂₆H₂₆F₄N₆O·0.25H₂O) C, H, N.

3-(2-(2-Aminopyrimidin-5-yl)ethynyl)-N-(2-(4-methylpiperazin-1-yl)-5-(trifluoromethyl)phenyl)benzamide (6i) was prepared according to general method A starting from 3-iodo-N-(2-(4-methylpiperazin-1-yl)-5-(trifluoromethyl)phenyl)benzamide (0.20 g, 0.39 mmol) to give **6i** (0.064 g, 33%) as a white solid: ¹H NMR (400 MHz, DMSO-*d*₆) δ ppm 9.89 (d, *J* = 8.3 Hz, 1 H), 8.59 (s, 1 H), 8.46 (s, 2 H), 8.01–8.07 (m, 1 H), 7.72–7.82 (m, 1 H), 7.41–7.60 (m, 3 H), 7.21 (s, 2 H), 3.09 (s, 3 H), 2.97 (s, 4 H), 2.60 (s, 3 H), 2.30 (s, 3 H), 1.08–1.27 (m, 5 H); HRMS *m/z* = 499.1872 [M + H]⁺, calcd [C₂₅H₂₂F₄N₆O + H]⁺ = 499.1864; HPLC *t*_R A, 6.32 min; B, 1.56 min.

5-(2-(2-Aminopyrimidin-5-yl)ethynyl)-*N*-(2-(4-(dimethylamino)piperidin-1-yl)-5-(trifluoromethyl)phenyl)-2-fluorobenzamide (6j) was prepared according to general method A starting from *N*-(2-(4-(dimethylamino)piperidin-1-yl)-5-(trifluoromethyl)phenyl)-2-fluoro-5-iodobenzamide (0.22 g, 0.40 mmol) to give **6j** (0.038 g, 18%) as a light yellow solid: $^1\text{H NMR}$ (400 MHz, DMSO- d_6) δ ppm 9.92 (d, $J = 8.5$ Hz, 1 H), 8.60 (s, 1 H), 8.46 (s, 2 H), 8.04 (d, $J = 5.9$ Hz, 1 H), 7.73–7.81 (m, 1 H), 7.42–7.56 (m, 3 H), 7.20 (s, 2 H), 3.09–3.18 (m, 2 H), 2.73 (t, $J = 10.9$ Hz, 2 H), 2.21 (s, 7 H), 1.85–1.93 (m, 2 H), 1.57–1.70 (m, 2 H); HRMS $m/z = 527.2188$ [M + H] $^+$, calcd [C₂₇H₂₆F₄N₆O + H] $^+$ = 527.2177. Anal. (C₂₇H₂₆F₄N₆O·0.75H₂O) C, H, N.

(*R*)-5-(2-(2-Aminopyrimidin-5-yl)ethynyl)-*N*-(2-(3-(dimethylamino)piperidin-1-yl)-5-(trifluoromethyl)phenyl)-2-fluorobenzamide (6k) was prepared according to general method A starting from (*R*)-*N*-(2-(3-(dimethylamino)piperidin-1-yl)-5-(trifluoromethyl)phenyl)-2-fluoro-5-iodobenzamide (0.22 g, 0.42 mmol), to give **6k** (0.18 g, 80%) as a off-white solid: $^1\text{H NMR}$ (400 MHz, DMSO- d_6) δ ppm 9.90 (d, $J = 8.0$ Hz, 1 H), 8.60 (s, 1 H), 8.46 (s, 2 H), 8.01–8.06 (m, 1 H), 7.72–7.84 (m, 1 H), 7.42–7.60 (m, 3 H), 7.21 (s, 2 H), 3.12 (d, $J = 11.1$ Hz, 1 H), 3.02 (d, $J = 11.0$ Hz, 1 H), 2.54–2.74 (m, 2 H), 2.38–2.48 (m, 1 H), 2.14 (s, 6 H), 1.86–1.97 (m, 1 H), 1.78–1.87 (m, 1 H), 1.61–1.75 (m, 1 H), 1.27–1.42 (m, 1 H); HRMS $m/z = 549.1999$ [M + Na] $^+$, calcd [C₂₇H₂₆F₄N₆O + Na] $^+$ = 549.1996. Anal. (C₂₇H₂₆F₄N₆O) C, H, N.

(*S*)-5-(2-(2-Aminopyrimidin-5-yl)ethynyl)-*N*-(2-(3-(dimethylamino)piperidin-1-yl)-5-(trifluoromethyl)phenyl)-2-fluorobenzamide (6l) was prepared according to general method A starting from (*S*)-*N*-(2-(3-(dimethylamino)piperidin-1-yl)-5-(trifluoromethyl)phenyl)-2-fluoro-5-iodobenzamide (0.15 g, 0.28 mmol), to give **6l** (0.096 g, 66%) as a off-white solid: $^1\text{H NMR}$ (400 MHz, DMSO- d_6) δ ppm 9.90 (d, $J = 8.0$ Hz, 1 H), 8.60 (s, 1 H), 8.46 (s, 2 H), 8.01–8.06 (m, 1 H), 7.72–7.84 (m, 1 H), 7.42–7.60 (m, 3 H), 7.21 (s, 2 H), 3.12 (d, $J = 11.1$ Hz, 1 H), 3.02 (d, $J = 11.0$ Hz, 1 H), 2.54–2.74 (m, 2 H), 2.38–2.48 (m, 1 H), 2.14 (s, 6 H), 1.86–1.97 (m, 1 H), 1.78–1.87 (m, 1 H), 1.61–1.75 (m, 1 H), 1.27–1.42 (m, 1 H); HRMS $m/z = 527.2191$ [M + H] $^+$, calcd [C₂₇H₂₆F₄N₆O + H] $^+$ = 527.2177. Anal. (C₂₇H₂₆F₄N₆O·0.25H₂O) C, H, N.

(*S*)-5-(2-(2-Aminopyrimidin-5-yl)ethynyl)-2-fluoro-*N*-(2-(3-(methylamino)piperidin-1-yl)-5-(trifluoromethyl)phenyl)benzamide (6m). In a 25-mL round-bottom flask, **9m** (0.496 g, 0.80 mmol), 5-ethynylpyrimidin-2-amine (0.19 g, 1.6 mmol), bis-(triphenylphosphine)palladium(II) dichloride (0.028 g, 0.040 mmol), and copper(I) iodide (0.0076 g, 0.040 mmol) were taken up in CH₃CN (10 mL) and triethylamine (1.7 mL). The reaction was flushed with nitrogen, sealed, and heated to 70 °C for 16 h. The reaction was cooled and transferred to a larger flask with EtOAc and concentrated under reduced pressure. The solid was adsorbed onto 4 g of silica gel from 10% MeOH/CH₂Cl₂, dried, and purified by silica gel chromatography (0–75% EtOAc/hexanes). Product-containing fractions were combined and concentrated to afford (*S*)-*tert*-butyl 1-(2-(5-(2-(2-aminopyrimidin-5-yl)ethynyl)-2-fluorobenzamido)-4-(trifluoromethyl)phenyl)piperidin-3-yl(methyl)carbamate (0.40 g, 81%) as an orange foam: $^1\text{H NMR}$ (400 MHz, DMSO- d_6) δ ppm 9.82–10.22 (m, 1 H), 8.61 (s, 1 H), 8.46 (s, 2 H), 8.07 (d, $J = 6.1$ Hz, 1 H), 7.72–7.83 (m, 1 H), 7.44–7.58 (m, 3 H), 7.21 (s, 2 H), 4.06–4.23 (m, 1 H), 2.97–3.13 (m, 1 H), 2.90 (d, $J = 7.7$ Hz, 2 H), 2.75 (s, 3 H), 2.54–2.67 (m, 1 H), 1.58–1.91 (m, 4 H), 1.33 (s, 9 H); MS $m/z = 613$ [M + H] $^+$, calcd for C₃₁H₃₂F₄N₆O₃ = 612.

To a yellow solution of (*S*)-*tert*-butyl 1-(2-(5-(2-(2-aminopyrimidin-5-yl)ethynyl)-2-fluorobenzamido)-4-(trifluoromethyl)phenyl)piperidin-3-yl(methyl)carbamate (1.5 g, 2.5 mmol) in 15 mL of CH₂Cl₂ at 0 °C was added TFA (0.94 mL, 12 mmol). The reaction was allowed to warm to ambient temperature and was stirred overnight. An additional 5 equiv of TFA was added, and after 3 days the reaction was cooled to 0 °C, and water was added, followed by basification with 1 N NaOH. The organic layer was separated, and the aqueous layer was extracted once with CH₂Cl₂. The combined organic layers were dried over anhydrous sodium sulfate,

filtered, and concentrated in vacuo to give **6m** (0.81 g, 65%) as a white solid: $^1\text{H NMR}$ (400 MHz, DMSO- d_6) δ ppm 8.57–8.63 (m, 1 H), 8.45 (s, 2 H), 7.97–8.07 (m, 1 H), 7.69–7.81 (m, 1 H), 7.46–7.57 (m, 2 H), 7.40 (d, $J = 8.3$ Hz, 1 H), 7.20 (s, 2 H), 3.01–3.13 (m, 1 H), 2.92–3.00 (m, 1 H), 2.69–2.81 (m, 1 H), 2.53–2.64 (m, 2 H), 2.09–2.22 (m, 3 H), 1.75–1.91 (m, 2 H), 1.59–1.71 (m, 1 H); HRMS $m/z = 535.1839$ [M + Na] $^+$, calcd [C₂₆H₂₄F₄N₆O + Na] $^+$ = 535.1840. Anal. (C₂₆H₂₄F₄N₆O·0.75H₂O) C, H, N.

(*S*)-*N*-(2-(3-Aminopiperidin-1-yl)-5-(trifluoromethyl)phenyl)-5-(2-(2-aminopyrimidin-5-yl)ethynyl)-2-fluorobenzamide (6n). To a slurry of **9n** (1.6 g, 2.6 mmol) in 5 mL of dioxane at 0 °C was added a solution of HCl (4.0 M in dioxane, 6.5 mL, 26 mmol). The clear yellow solution was allowed to warm to ambient temperature and was stirred for 1 h. The reaction was concentrated in vacuo to give (*S*)-*N*-(2-(3-aminopiperidin-1-yl)-5-(trifluoromethyl)phenyl)-2-fluoro-5-iodobenzamide dihydrochloride (1.6 g, quant.) as a peach-colored solid: $^1\text{H NMR}$ (400 MHz, DMSO- d_6) δ ppm 9.96 (d, $J = 3.2$ Hz, 1 H), 8.48 (s, 1 H), 8.20 (s, 3 H), 8.12 (dd, $J = 6.6, 2.2$ Hz, 1 H), 7.91–8.00 (m, 1 H), 7.54 (dd, $J = 8.3, 1.6$ Hz, 1 H), 7.35 (d, $J = 8.5$ Hz, 1 H), 7.26 (dd, $J = 10.3, 10.3$ Hz, 1 H), 3.50 (s, 1 H), 3.22–3.32 (m, 1 H), 3.02–3.13 (m, 1 H), 2.91–3.00 (m, 1 H), 2.64–2.76 (m, 1 H), 1.61–2.01 (m, 4 H); MS $m/z = 508$ (M + H) $^+$, calcd for C₁₉H₁₈F₄N₃O = 507.

In a 16 × 120 mm resealable pyrex tube, (*S*)-*N*-(2-(3-aminopiperidin-1-yl)-5-(trifluoromethyl)phenyl)-2-fluoro-5-iodobenzamide dihydrochloride (0.25 g, 0.43 mmol), 5-ethynylpyrimidin-2-amine (0.10 g, 0.86 mmol), bis(triphenylphosphine)palladium(II) dichloride (0.015 g, 0.022 mmol), and copper(I) iodide (0.0041 g, 0.022 mmol) were taken up in CH₃CN (5 mL) and triethylamine (0.91 mL), and the tube was flushed with nitrogen. The tube was sealed and the reaction heated to 70 °C for 3 h. The reaction was cooled, diluted with EtOAc, and filtered through a pad of Celite with rinsing with 100 mL of EtOAc. The resulting clear yellow solution was extracted twice with 1 N NaOH, dried over anhydrous sodium sulfate, filtered, and concentrated to an orange oil. The material was dissolved in a minimal amount of CH₂Cl₂ and purified by silica gel chromatography (0–100% 90/10/1 CH₂Cl₂/MeOH/concentrated NH₄OH in CH₂Cl₂). The product-containing fractions were combined and concentrated to afford **6n** (0.13 g, 61%) as a pale yellow solid: $^1\text{H NMR}$ (400 MHz, DMSO- d_6) δ ppm 8.62 (s, 1 H), 8.46 (s, 2 H), 7.98–8.08 (m, 1 H), 7.73–7.80 (m, 1 H), 7.46–7.56 (m, 2 H), 7.40 (d, $J = 8.0$ Hz, 1 H), 7.20 (s, 2 H), 3.17 (d, $J = 2.9$ Hz, 1 H), 2.99–3.06 (m, 1 H), 2.85–2.96 (m, 2 H), 2.64–2.77 (m, 1 H), 2.39–2.48 (m, 1 H), 1.76–1.90 (m, 2 H), 1.58–1.72 (m, 1 H), 1.12–1.27 (m, 1 H); HRMS $m/z = 499.1866$ [M + H] $^+$, calcd [C₂₆H₂₄F₄N₆O + H] $^+$ = 499.1864. Anal. (C₂₅H₂₂F₄N₆O·1.7H₂O) C, H, N.

(*R*)-5-(2-(2-Aminopyrimidin-5-yl)ethynyl)-*N*-(2-(3-(dimethylamino)pyrrolidin-1-yl)-5-(trifluoromethyl)phenyl)-2-fluorobenzamide (6o) was prepared according to general method A starting from (*R*)-*N*-(2-(3-(dimethylamino)pyrrolidin-1-yl)-5-(trifluoromethyl)phenyl)-2-fluoro-5-iodobenzamide (0.25 g, 0.45 mmol) to give **6o** (0.041 g, 18%) as an off white solid: $^1\text{H NMR}$ (400 MHz, DMSO- d_6) δ ppm 10.10 (s, 1 H), 8.44 (s, 2 H), 7.88 (dd, $J = 7.0, 2.2$ Hz, 1 H), 7.66–7.74 (m, 1 H), 7.49 (d, $J = 2.2$ Hz, 1 H), 7.38–7.46 (m, 2 H), 7.21 (s, 2 H), 6.88 (d, $J = 8.8$ Hz, 1 H), 3.47–3.56 (m, 1 H), 3.37–3.47 (m, 2 H), 3.25–3.33 (m, 1 H), 2.59–2.72 (m, 1 H), 2.15 (s, 6 H), 2.04–2.13 (m, 1 H), 1.62–1.76 (m, 1 H); HRMS $m/z = 535.1842$ [M + Na] $^+$, calcd [C₂₆H₂₄F₄N₆O + Na] $^+$ = 535.1840; HPLC t_R A, 6.80 min; C, 4.69 min.

(*S*)-5-(2-(2-Aminopyrimidin-5-yl)ethynyl)-*N*-(2-(3-(dimethylamino)pyrrolidin-1-yl)-5-(trifluoromethyl)phenyl)-2-fluorobenzamide (6p) was prepared according to general method A starting from (*S*)-*N*-(2-(3-(dimethylamino)pyrrolidin-1-yl)-5-(trifluoromethyl)phenyl)-2-fluoro-5-iodobenzamide (0.15 g, 0.288 mmol) to give **6p** (0.092 g, 61%) as an off-white solid: $^1\text{H NMR}$ (400 MHz, DMSO- d_6) δ ppm 10.10 (s, 1 H), 8.44 (s, 2 H), 7.88 (dd, $J = 7.0, 2.2$ Hz, 1 H), 7.66–7.74 (m, 1 H), 7.49 (d, $J = 2.2$ Hz, 1 H), 7.38–7.46 (m, 2 H), 7.21 (s, 2 H), 6.88 (d, $J = 8.8$ Hz, 1 H), 3.47–3.56 (m, 1 H), 3.37–3.47 (m, 2 H), 3.25–3.33 (m, 1 H), 2.59–2.72 (m, 1

H), 2.15 (s, 6 H), 2.04–2.13 (m, 1 H), 1.62–1.76 (m, 1 H); HRMS $m/z = 535.1838$ [M + Na]⁺, calcd [C₂₆H₂₄F₄N₆O + Na]⁺ = 535.1840. Anal. (C₂₆H₂₄F₄N₆O·0.1CH₂Cl₂) C, H, N.

1-(2-Amino-4-(trifluoromethyl)phenyl)-N,N-dimethylpiperidin-4-amine (8j). To **15j** (3.4 g, 11 mmol) was added Pd/C (10%, 0.57 g) under nitrogen. Methanol (25 mL) was added via syringe, H₂ gas was introduced, and the mixture was stirred vigorously under an atmosphere of H₂. After 96 h, the mixture was flushed with nitrogen, filtered through Celite, and concentrated. The residue was resubjected to the reaction conditions. After 12 h, the reaction was flushed with nitrogen, filtered through Celite and concentrated. The resulting solid was triturated with methanol 10 times to give **8j** (0.67 g, 22%) as a pink solid: ¹H NMR (400 MHz, DMSO-*d*₆) δ ppm 8.12 (d, *J* = 1.8 Hz, 1 H), 7.82 (dd *J* = 2.2, 8.8 Hz, 1 H), 7.41 (d, *J* = 8.8 Hz, 1 H), 3.33–3.36 (m, 2 H), 2.94 (dd, *J* = 11.7 Hz, 2 H), 2.28–2.30 (m, 1 H), 1.80–1.83 (m, 2 H), 1.47 (ddd, *J* = 3.7, 12.5, 12.5 Hz, 2 H); MS $m/z = 288.2$ (M + H)⁺, calcd for C₁₄H₂₀F₃N₃ = 287.3.

(R)-1-(2-Amino-4-(trifluoromethyl)phenyl)-N,N-dimethylpiperidin-3-amine (8k) was synthesized in a manner analogous to **8l** but starting from **15k** (1.0 g, 2.6 mmol) to give **8k** (0.80 g, quant., three steps) as a red oil, which was used without further purification: ¹H NMR (400 MHz, DMSO-*d*₆) δ ppm 7.01 (d, *J* = 8.1 Hz, 1 H), 6.95 (d, *J* = 1.9 Hz, 1 H), 6.83 (d, *J* = 8.1 Hz, 1 H), 5.08 (s, 2 H), 3.21 (d, *J* = 10.7 Hz, 1 H), 3.02 (d, *J* = 11.5 Hz, 1 H), 2.29–2.47 (m, 3 H), 2.21 (s, 6 H), 1.85–1.95 (m, 1 H), 1.72–1.81 (m, 1 H), 1.58–1.72 (m, 1 H), 1.17–1.36 (m, 1 H); MS $m/z = 288$ [M + H]⁺, calcd for C₁₄H₂₀F₃N₃ = 287.

(S)-1-(2-Amino-4-(trifluoromethyl)phenyl)-N,N-dimethylpiperidin-3-amine (8l). A solution of **15l** (15.6 g, 40 mmol) was cooled to 0 °C, hydrochloric acid (4.0 M in dioxane, 80 mL, 321 mmol) was added, and the mixture was allowed to warm to ambient temperature. The orange solution was allowed to stir for 14 h, at which point it was concentrated in vacuo to give (S)-1-(2-nitro-4-(trifluoromethyl)phenyl)piperidin-3-amine dihydrochloride (13.4 g, 92%) as a yellow solid: ¹H NMR (400 MHz, DMSO-*d*₆) δ ppm 9.96 (d, *J* = 3.2 Hz, 1 H), 8.47 (s, 1 H), 8.20 (s, 3 H), 8.12 (dd, *J* = 6.6, 2.2 Hz, 1 H), 7.90–8.00 (m, 1 H), 7.53 (dd, *J* = 8.4, 1.8 Hz, 1 H), 7.34 (d, *J* = 8.5 Hz, 1 H), 7.20–7.30 (m, 1 H), 3.43–3.54 (m, 1 H), 3.26 (dd, *J* = 11.6, 2.4 Hz, 1 H), 3.00–3.14 (m, 1 H), 2.94 (dd, *J* = 11.5, 5.3 Hz, 1 H), 2.64–2.76 (m, 1 H), 1.81–2.00 (m, 2 H), 1.61–1.80 (m, 2 H); MS $m/z = 290.0$ [M + H]⁺, calcd for C₁₂H₁₄F₃N₃O₂ = 289.

To a yellow solution of (S)-1-(2-nitro-4-(trifluoromethyl)phenyl)piperidin-3-amine dihydrochloride (13.4 g, 37 mmol) in 123 mL of MeOH under nitrogen at 0 °C were added formaldehyde (37% solution) (14 mL, 185 mmol), acetic acid (11 mL, 185 mmol), and sodium cyanoborohydride (4.6 g, 74 mmol) in portions over 5 min. The cloudy mixture was warmed to ambient temperature. After 10 min, the reaction became quite hot and was cooled with an ice bath. The reaction was allowed to warm to ambient temperature, and after 1.5 h, the reaction was judged complete by LC–MS. The solvent was removed under reduced pressure, and the flask cooled to 0 °C. Water was added, and the mixture was basified with 1 N NaOH and 6 N NaOH. The mixture was extracted with 1 × 200 mL EtOAc and 1 × 100 mL EtOAc, and the combined organics were dried over anhydrous Na₂SO₄ and concentrated under reduced pressure to give (S)-N,N-dimethyl-1-(2-nitro-4-(trifluoromethyl)phenyl)piperidin-3-amine (13.6 g, quant.) as an orange oil, which was used without further purification: ¹H NMR (400 MHz, DMSO-*d*₆) δ ppm 8.59 (s, 1 H), 8.45 (s, 2 H), 7.98–8.05 (m, 1 H), 7.71–7.80 (m, 1 H), 7.44–7.54 (m, 2 H), 7.40 (d, *J* = 8.5 Hz, 1 H), 3.07 (d, *J* = 10.1 Hz, 1 H), 2.87–2.98 (m, 1 H), 2.70–2.80 (m, 1 H), 2.53–2.65 (m, 2 H), 2.14 (s, 3 H), 1.76–1.89 (m, 2 H), 1.58–1.71 (m, 1 H); MS $m/z = 318$ [M + H]⁺, calcd for C₁₄H₁₈F₃N₃O₂ = 317.

A 500-mL Parr pressure bottle was charged with palladium, 10 wt % on activated carbon, 50% water (9.1 g) under nitrogen. (S)-N,N-Dimethyl-1-(2-nitro-4-(trifluoromethyl)phenyl)piperidin-3-amine (13.6 g, 43 mmol) was added as a solution in methanol via syringe, rinsing in with multiple methanol washes until the final

volume was approximately 100 mL. The vessel was placed in a Parr shaker, treated with 2 atm H₂, and shaken overnight. The reaction was flushed with nitrogen, and filtered through a pad of Celite rinsing with 1.3 L of methanol, and the filtrate was concentrated under reduced pressure. The oil was taken up in CH₂Cl₂, dried over Na₂SO₄, filtered, and concentrated under reduced pressure to give **8l** (12.1 g, 98%) as a red oil, which was used without further purification: ¹H NMR (400 MHz, DMSO-*d*₆) δ ppm 7.01 (d, *J* = 8.1 Hz, 1 H), 6.95 (d, *J* = 1.9 Hz, 1 H), 6.83 (d, *J* = 8.1 Hz, 1 H), 5.08 (s, 2 H), 3.21 (d, *J* = 10.7 Hz, 1 H), 3.02 (d, *J* = 11.5 Hz, 1 H), 2.29–2.47 (m, 3 H), 2.21 (s, 6 H), 1.85–1.95 (m, 1 H), 1.72–1.81 (m, 1 H), 1.58–1.72 (m, 1 H), 1.17–1.36 (m, 1 H); MS $m/z = 288$ [M + H]⁺, calcd for C₁₄H₂₀F₃N₃ = 287.

(S)-tert-Butyl 1-(2-(2-Fluoro-5-iodobenzamido)-4-(trifluoromethyl)phenyl)piperidin-3-ylcarbamate (9n). To a 100-mL round-bottom flask was added **15l** (1.0 g, 2.6 mmol) and palladium, 10 wt % on activated carbon, 50% water (0.55 g) under nitrogen. Methanol (10 mL) was added via syringe, and the atmosphere was purged with hydrogen from a balloon. The reaction was allowed to stir rapidly under hydrogen for 24 h. The flask was purged with nitrogen, filtered through Celite, rinsing with 100 mL of MeOH, and concentrated to give (S)-tert-butyl 1-(2-amino-4-(trifluoromethyl)phenyl)piperidin-3-ylcarbamate (0.92 g, 99%) as a gray solid, which was used without further purification: ¹H NMR (400 MHz, DMSO-*d*₆) δ ppm 8.03–8.15 (m, 3 H), 7.93 (d, *J* = 9.6 Hz, 1 H), 6.32 (s, 2 H), 4.68–4.86 (m, 1 H), 4.16 (d, *J* = 13.1 Hz, 1 H), 3.86–3.96 (m, 1 H), 3.65–3.74 (m, 1 H), 3.47–3.57 (m, 1 H), 2.81–3.04 (m, 2 H), 2.66–2.77 (m, 1 H), 2.49–2.50 (s, 9 H), 2.37–2.60 (m, 1 H); MS $m/z = 360$ [M + H]⁺, calcd for C₁₇H₂₄F₃N₃O₂ = 359.

In a screw-cap vial, (S)-tert-butyl 1-(2-amino-4-(trifluoromethyl)phenyl)piperidin-3-ylcarbamate (0.915 g, 2.5 mmol) was taken up in dichloromethane (5 mL). Triethylamine (0.47 mL, 3.3 mmol) and 2-fluoro-5-iodobenzoyl chloride (0.80 g, 2.8 mmol) were then added. The tube was sealed and the reaction stirred overnight. The reaction mixture was poured into EtOAc/saturated aqueous sodium bicarbonate. The organic layer was dried over anhydrous sodium sulfate and concentrated in vacuo. The resulting foam **9n** (1.59 g, quant.) was used without further purification: ¹H NMR (400 MHz, DMSO-*d*₆) δ ppm 9.90 (d, *J* = 6.4 Hz, 1 H), 8.48 (s, 1 H), 8.19 (d, *J* = 5.4 Hz, 1 H), 7.93–8.03 (m, 1 H), 7.51 (d, *J* = 8.3 Hz, 1 H), 7.36 (d, *J* = 8.6 Hz, 1 H), 7.28 (dd, *J* = 10.5, 9.2 Hz, 1 H), 6.97 (d, *J* = 7.8 Hz, 1 H), 3.57–3.73 (m, 1 H), 3.04–3.20 (m, 1 H), 2.84–2.97 (m, 1 H), 2.61–2.76 (m, 1 H), 2.51–2.60 (m, 1 H), 1.74–1.87 (m, 2 H), 1.60–1.72 (m, 1 H), 1.34 (s, 9 H), 1.22–1.47 (m, 1 H); MS $m/z = 608$ [M + H]⁺, calcd for C₂₄H₂₆F₄IN₃O₃ = 607.

(S)-tert-Butyl 1-(2-(2-Fluoro-5-iodobenzamido)-4-(trifluoromethyl)phenyl)piperidine-3-carboxylate (9m). To a 100-mL round-bottom flask were added **15m** (1.8 g, 4.3 mmol) and palladium, 10 wt. % on activated carbon, 50% water (0.92 g) under nitrogen. MeOH (12 mL) was added via syringe, and the atmosphere was purged with hydrogen from a balloon. The reaction was allowed to stir rapidly under hydrogen for 8 h. The flask was purged with nitrogen, filtered through Celite, with rinsing with 100 mL of MeOH, and concentrated to give (S)-tert-butyl 1-(2-amino-4-(trifluoromethyl)phenyl)piperidin-3-yl(methyl)carbamate (1.44 g, 89%) as a gray solid, which was used without further purification: ¹H NMR (400 MHz, DMSO-*d*₆) δ ppm 7.02 (d, *J* = 8.1 Hz, 1 H) 6.96 (d, *J* = 1.8 Hz, 1 H) 6.83 (d, *J* = 8.0 Hz, 1 H) 5.11 (s, 2 H) 3.92–4.19 (m, 1 H) 2.86–3.15 (m, 2 H) 2.74 (s, 3 H) 2.57–2.69 (m, 1 H) 2.28–2.47 (m, 1 H) 1.50–1.85 (m, 4 H) 1.40 (s, 9 H); MS $m/z = 374$ [M + H]⁺, calcd for C₁₈H₂₆F₃N₃O₂ = 373.

In a vial, (S)-tert-butyl 1-(2-amino-4-(trifluoromethyl)phenyl)piperidin-3-yl(methyl)carbamate (0.500 g, 1.3 mmol) was taken up in CH₂Cl₂ (5 mL). The solution was cooled to 0 °C and triethylamine (0.24 mL, 1.7 mmol) and 2-fluoro-5-iodobenzoyl chloride (0.42 g, 1.5 mmol) were then added. The tube was sealed and the reaction stirred for 2 h. The reaction mixture was poured into EtOAc/1 N NaOH. The organic layer was dried over anhydrous

sodium sulfate and concentrated in vacuo. The resulting off-white foam **9m** (0.91 g, quant.) was used without further purification: ¹H NMR (400 MHz, DMSO-*d*₆) δ ppm 9.70–10.19 (m, 1 H), 8.57 (s, 1 H), 8.23 (d, *J* = 2.1 Hz, 1 H), 7.90–8.08 (m, 1 H), 7.42–7.60 (m, 2 H), 7.28 (dd, *J* = 11.2, 8.8 Hz, 1 H), 4.04–4.22 (m, 1 H), 2.97–3.14 (m, 1 H), 2.89 (d, *J* = 6.8 Hz, 2 H), 2.74 (s, 3 H), 2.52–2.65 (m, 1 H), 1.55–1.89 (m, 4 H), 1.33 (s, 9 H); MS *m/z* = 622 [M + H]⁺, calcd for C₂₅H₂₈F₄IN₃O₃ = 621.

5-Ethynylpyrimidin-2-amine (11). Into a 1-L round-bottom flask were placed 2-amino-5-iodopyrimidine (8.0 g, 36 mmol), acetonitrile (300 mL), triethylamine (30 mL), TMS-acetylene (7.7 g, 78 mmol), PdCl₂(PPh₃)₂ (1.3 g, 1.8 mmol), and CuI (0.34 g, 1.8 mmol). The vessel was filled with argon and allowed to stir at room temperature for 3 h. The solvent was evaporated and the material was taken up in methanol (400 mL). Excess potassium carbonate (10 equiv) was added, and the mixture was stirred at room temperature for 1.5 h. Activated charcoal was added and the mixture was filtered through Celite. The filtrate was concentrated under reduced pressure to afford a tan solid, which was added to a solution of 10% methanol in water (200 mL). The resulting precipitate was isolated by filtration and dried in a vacuum oven to constant mass to afford **11** (3.5 g, 81%) as a tan solid: ¹H NMR (400 MHz, CDCl₃) δ ppm 8.43 (s, 2H), 5.21 (br s, 2H), 3.20 (s, 1H); MS *m/z* = 120 [M + H]⁺, calcd for C₆H₅N₃ = 119.

3-Ethynyl-4-methyl-*N*-(3-(trifluoromethyl)phenyl)benzamide (12) was prepared according to general method B starting with 3-iodo-4-methyl-*N*-(3-(trifluoromethyl)phenyl)benzamide (1.5 g, 3.7 mmol) to afford **12** (0.44 g, 91%) as an off white solid: ¹H NMR (400 MHz, DMSO-*d*₆) δ ppm: 10.55 (s, 1H), 8.24 (br s, 1H), 8.10 (d, *J* = 1.90 Hz), 8.06 (d, *J* = 9.06 Hz), 7.91 (dd, *J* = 8.04, 1.90 Hz), 7.61 (t, *J* = 7.97 Hz), 7.43–7.51 (m, 2H), 4.55 (s, 1H), 2.47 (s, 3H); MS *m/z* = 302 [M – H][–], calcd for C₁₇H₁₂NO = 303.

3-(2-(6-Aminopyridin-3-yl)ethynyl)-4-methyl-*N*-(3-(trifluoromethyl)phenyl)benzamide (13a) was prepared according to general method B starting from 3-ethynyl-4-methyl-*N*-(3-(trifluoromethyl)phenyl)benzamide (0.050 g, 0.33 mmol) to give **13a** (0.009 g, 7%) as an off white solid: ¹H NMR (400 MHz, DMSO-*d*₆) δ ppm 10.55 (s, 1 H), 8.25 (s, 1 H), 8.17 (s, 1 H), 8.02–8.12 (m, 2 H), 7.86 (d, *J* = 8.0 Hz, 1 H), 7.60 (t, *J* = 6.9 Hz, 1 H), 7.55 (d, *J* = 8.0 Hz, 1 H), 7.41–7.51 (m, 2 H), 6.48 (s, 2 H), 3.33 (s, 3 H); HRMS *m/z* = 396.1326 [M + H]⁺, calcd [C₂₂H₁₆F₃N₃O + H]⁺ = 396.1318; HPLC *t*_R A, 7.39 min; B, 1.84 min.

3-(2-(3*H*-Imidazo[4,5-*b*]pyridin-6-yl)ethynyl)-4-methyl-*N*-(3-(trifluoromethyl)phenyl)benzamide (13b) was prepared according to general method B starting from 3-ethynyl-4-methyl-*N*-(3-(trifluoromethyl)phenyl)benzamide (0.15 g, 0.48 mmol) and 6-bromo-3*H*-imidazo[4,5-*b*]pyridine²⁸ (0.070 g, 0.37 mmol) to give **13b** as a tan solid (0.031 g, 20%): ¹H NMR (400 MHz, DMSO-*d*₆) δ ppm 10.60 (s, 1 H), 8.61 (s, 1 H), 8.57 (s, 1 H), 8.23–8.33 (m, 2 H), 8.20 (s, 1 H), 8.09 (d, *J* = 7.7 Hz, 1 H), 7.93 (d, *J* = 8.1 Hz, 1 H), 7.61 (t, *J* = 8.1 Hz, 1 H), 7.54 (d, 1 H), 7.47 (d, *J* = 8.1 Hz, 1 H), 2.59 (s, 3 H); HRMS *m/z* = 421.1275 [M + H]⁺, calcd [C₂₃H₁₅F₃N₄O + H]⁺ = 421.1271; HPLC *t*_R A, 8.14 min; B, 2.10 min.

***N*-Methyl-5-(2-(2-methyl-5-(3-(trifluoromethyl)phenyl)carbamoyl)phenyl)ethynyl)picolinamide (13c)** was prepared according to general method B starting from 3-ethynyl-4-methyl-*N*-(3-(trifluoromethyl)phenyl)benzamide (0.16 g, 0.54 mmol) and 5-bromo-*N*-methylpicolinamide²⁹ (0.089 g, 0.41 mmol) to give **13c** as a white solid (0.086 g, 48%): ¹H NMR (400 MHz, acetone-*d*₆) δ ppm 9.89 (s, 1 H), 8.79 (s, 1 H), 8.38 (s, 1 H), 8.33 (s, 1 H), 8.21 (d, *J* = 1.5 Hz, 1 H), 8.17 (s, 2 H), 8.12 (d, *J* = 8.1 Hz, 1 H), 8.01 (dd, *J* = 7.9, 1.6 Hz, 1 H), 7.61 (t, *J* = 7.9 Hz, 1 H), 7.52 (d, *J* = 8.1 Hz, 1 H), 7.47 (d, *J* = 7.7 Hz, 1 H), 2.98 (d, *J* = 4.8 Hz, 3 H), 2.61 (s, 3 H); HRMS *m/z* = 460.1247 [M + Na]⁺, calcd [C₂₄H₁₈F₃N₃O₂ + Na]⁺ = 460.1243. Anal. (C₂₄H₁₈F₃N₃O₂·0.75H₂O) C, H, N.

4-Methyl-3-(2-(quinolin-3-yl)ethynyl)-*N*-(3-(trifluoromethyl)phenyl)benzamide (13d) was prepared according to general method A starting from 3-iodo-4-methyl-*N*-(3-(trifluoromethyl)phenyl)benzamide (0.32 g, 0.80 mmol) and 3-ethynylquinoline³⁰ (0.16 g,

1.0 mmol) to give **13d** as white solid (0.18 g, 51%): ¹H NMR (400 MHz, acetone-*d*₆) δ ppm 9.90 (s, 1 H), 9.04 (s, 1 H), 8.57 (s, 1 H), 8.34 (s, 1 H), 8.24 (s, 1 H), 8.13 (d, *J* = 8.4 Hz, 1 H), 8.09 (d, *J* = 8.4 Hz, 1 H), 8.00 (t, *J* = 7.3 Hz, 2 H), 7.82 (t, *J* = 7.1 Hz, 1 H), 7.68 (t, *J* = 7.5 Hz, 1 H), 7.61 (t, *J* = 7.9 Hz, 1 H), 7.52 (d, *J* = 8.1 Hz, 1 H), 7.47 (d, *J* = 7.7 Hz, 1 H), 2.59–2.69 (m, 3 H); HRMS *m/z* = 431.1376 [M + H]⁺, calcd [C₂₆H₁₇F₃N₂O + H]⁺ = 431.1366. Anal. (C₂₆H₁₇F₃N₂O) C, H, N.

4-Methyl-3-(2-(quinoxalin-2-yl)ethynyl)-*N*-(3-(trifluoromethyl)phenyl)benzamide (13e) was prepared according to general method B starting from 3-ethynyl-4-methyl-*N*-(3-(trifluoromethyl)phenyl)benzamide (0.17 g, 0.57 mmol) and 2-bromoquinoxaline³¹ (0.080 g, 0.38 mmol) to afford **13e** as a white solid (0.15 g, 92%): ¹H NMR (300 MHz, acetone-*d*₆) ppm 9.94 (s, 1 H), 9.00–9.19 (m, 1 H), 8.34–8.37 (m, 1 H), 8.33 (d, *J* = 2.2 Hz, 1 H), 8.13–8.16 (m, 1 H), 8.10–8.13 (m, 1 H), 8.07–8.10 (m, 1 H), 8.05 (d, *J* = 1.9 Hz, 1 H), 7.87–7.97 (m, 2 H), 7.54–7.66 (m, 2 H), 7.47 (d, *J* = 7.7 Hz, 1 H), 2.69 (s, 3 H); HRMS *m/z* = 432.1319 [M + H]⁺, calcd [C₂₆H₁₇F₃N₂O + H]⁺ = 432.1318; HPLC *t*_R A, 10.11 min; B, 2.30 min.

***N,N*-Dimethyl-1-(2-nitro-4-(trifluoromethyl)phenyl)piperidin-4-amine (15j).** To a mixture of 4-amino-1-benzylpiperidine (5.0 g, 26 mmol), NaBH₃CN (3.3 g, 53 mmol), AcOH (7.5 mL, 132 mmol) in 130 mL of MeOH at 0 °C under nitrogen was added formaldehyde (37 wt % in water, 5.3 mL) as a solution in 15 mL of MeOH slowly dropwise via a pressure-equalized addition funnel over 15 min. The resulting clear solution was allowed to warm to ambient temperature and was allowed to stir for approximately 60 h. The reaction was quenched by the addition of 20 mL of saturated aqueous potassium carbonate. The mixture was concentrated under reduced pressure, and water and EtOAc were added. The organic layer was removed, and the aqueous layer was extracted twice with EtOAc. The combined organic layers were dried with Na₂SO₄, filtered, and concentrated to give a cloudy oil, which was dissolved in methylene chloride and filtered through a fritted funnel. The solvent was removed to give a waxy solid, which was purified by silica gel chromatography (DCM/MeOH/concentrated NH₄OH). The resulting material was dissolved in diethyl ether, cooled to 0 °C, and treated with 20 mL of 4 N HCl in dioxane. The solvent was removed in vacuo to give 1-benzyl-*N,N*-dimethylpiperidin-4-amine dihydrochloride (7.02 g, 92%) as a white solid: MS *m/z* = 219.1 (M + H)⁺, calcd for C₁₄H₂₂N₂ = 218.3.

To 1-benzyl-*N,N*-dimethylpiperidin-4-amine dihydrochloride (6.7 g, 23 mmol) was added Pd/C (10%, 2.4 g) under argon. Methanol (100 mL) was added via syringe, H₂ gas was introduced, and the mixture was stirred vigorously under an atmosphere of H₂. After 48 h, the mixture was flushed with nitrogen, filtered through Celite, and concentrated to afford a mixture of starting material and *N,N*-dimethylpiperidin-4-amine dihydrochloride as a white solid. This solid was treated with 1-fluoro-2-nitro-4-trifluoromethylbenzene (3.2 mL, 23 mmol), triethylamine (13 mL, 92 mmol), and 50 mL of THF. The reaction was fitted with a water-cooled reflux condenser and the mixture was heated to 75 °C for 12 h. The mixture was allowed to cool to ambient temperature, filtered through a fritted funnel, and concentrated to an orange oil. The residue was purified by silica gel chromatography (DCM/MeOH/concentrated NH₄OH) to give **15j** (3.4 g, 47%) as an orange oil: ¹H NMR (400 MHz, DMSO-*d*₆) δ ppm 6.98 (d, *J* = 7.7 Hz, 1 H), 6.94 (s, 1 H), 6.82 (d, *J* = 8.1 Hz, 1 H), 5.11 (s, 2 H), 3.15 (d, *J* = 11.0 Hz, 2 H), 2.41–2.57 (m, 2 H), 2.20 (s, 6 H), 2.10–2.29 (m, 1 H), 1.82 (d, *J* = 11.0 Hz, 2 H), 1.52–1.68 (m, 2 H); MS *m/z* = 318.1 (M + H)⁺, calcd for C₁₄H₁₈F₃N₃O₂ = 317.3.

(*R*)-*tert*-Butyl 1-(2-nitro-4-(trifluoromethyl)phenyl)piperidin-3-ylcarbamate (15k) was prepared in an analogous manner to **15i** starting with (*R*)-3-*N*-Boc-aminopiperidine (0.97 g, 4.5 mmol) to give **15k** (1.8 g, 94%) as an orange solid: ¹H NMR (400 MHz, DMSO-*d*₆) δ ppm 8.11 (s, 1 H), 7.83 (d, *J* = 8.3 Hz, 1 H), 7.41 (d, *J* = 8.8 Hz, 1 H), 6.94 (d, *J* = 6.6 Hz, 1 H), 3.40–3.51 (m, 1 H), 3.28–3.34 (m, 1 H), 3.13–3.22 (m, 1 H), 2.92 (dd, *J* = 10.4 Hz, 1 H), 2.79 (dd, *J* = 10.6, 10.6 Hz, 1 H), 1.80–1.91 (m, 1 H), 1.71–

1.80 (m, 1 H), 1.47–1.63 (m, 1 H), 1.37 (s, 9 H), 1.25–1.46 (m, 1 H); MS m/z = 390 [M + H]⁺, calcd for C₁₇H₂₀F₃N₃ = 389.

(S)-tert-Butyl 1-(2-Nitro-4-(trifluoromethyl)phenyl)piperidin-3-ylcarbamate (15l). To a 200-mL round-bottom flask were added (S)-3-*N*-Boc-aminopiperidine (10.9 g, 54.4 mmol), sodium bicarbonate (11.4 g, 136 mmol), THF (100 mL), and 1-fluoro-2-nitro-4-(trifluoromethyl)benzene (7.62 mL, 54.4 mmol). The reaction was fitted with a water-cooled reflux condenser and the yellow mixture was heated to 70 °C. After 14 h, the mixture was cooled to ambient temperature and filtered through a glass frit, with rinsing with EtOAc. Concentration under reduced pressure afforded an orange oil, which crystallized on standing to an orange solid. The material was treated with 250 mL of hexanes and heated to 60 °C. Small amounts of EtOAc were added until all solid dissolved, with a total volume of 10 mL of EtOAc. The solution was allowed to cool overnight, resulting in the formation of orange crystals. The liquid was decanted, and the crystals were rinsed twice with 50 mL of hexanes. The crystals were collected, and the filtrate was concentrated to an orange solid, which was recrystallized to give a total of **15l** (18.3 g, 86%) as orange crystals: ¹H NMR (400 MHz, DMSO-*d*₆) δ ppm 8.11 (s, 1 H), 7.83 (d, *J* = 8.3 Hz, 1 H), 7.41 (d, *J* = 8.8 Hz, 1 H), 6.94 (d, *J* = 6.6 Hz, 1 H), 3.40–3.51 (m, 1 H), 3.28–3.34 (m, 1 H), 3.13–3.22 (m, 1 H), 2.92 (dd, *J* = 10.4 Hz, 1 H), 2.79 (dd, *J* = 10.6, 10.6 Hz, 1 H), 1.80–1.91 (m, 1 H), 1.71–1.80 (m, 1 H), 1.47–1.63 (m, 1 H), 1.37 (s, 9 H), 1.25–1.46 (m, 1 H); MS m/z = 390 [M + H]⁺, calcd for C₁₇H₂₀F₃N₃ = 389.

(S)-tert-Butyl Methyl(1-(2-nitro-4-(trifluoromethyl)phenyl)piperidin-3-yl)carbamate (15m). To an orange solution of (S)-tert-butyl 1-(2-nitro-4-(trifluoromethyl)phenyl)piperidin-3-ylcarbamate (1.5 g, 3.9 mmol) in DMF (13 mL) at 0 °C was added sodium hydride as a 60% dispersion in mineral oil (0.19 g, 4.8 mmol). Bubbling was observed, and the solution became darker orange. After 20 min, iodomethane (0.30 mL, 4.8 mmol) was added dropwise via syringe. The orange mixture was allowed to warm to room temperature over 30 min. Water was added, followed by diethyl ether. The organics were washed once with water and with brine, dried over anhydrous sodium sulfate, filtered, and concentrated under reduced pressure to give **15m** (1.8 g, quant.) as an orange semisolid which was used without further purification: ¹H NMR (400 MHz, DMSO-*d*₆) δ ppm 8.14 (s, 1 H), 7.84 (d, *J* = 8.2 Hz, 1 H), 7.45 (d, *J* = 9.0 Hz, 1 H), 3.82–3.99 (m, 1 H), 3.02–3.30 (m, 3 H), 2.87–2.95 (m, 1 H), 2.74 (s, 3 H), 1.51–1.85 (m, 4 H), 1.40 (s, 9 H); MS m/z = 404 [M + H]⁺, calcd for C₁₈H₂₄F₃N₃O₄ = 403.

Solubility Determination. Aqueous solubility was determined according to an automated procedure.³²

Plasma Protein Binding. Mouse plasma protein binding was determined in filtered mouse plasma by ultrafiltration³³ at 37 °C with a 10 μM concentration of **6l**.

Microsomal Incubations. Rat and mouse liver microsomes were incubated at 0.1 mg/mL protein, 1.0 μM substrate, and 1 mM NADPH in pH 7.4 phosphate buffer at 37 °C. The reaction was stopped with 0.5% formic acid in acetonitrile at 0, 5, 15, 30, and 45 min and analyzed by LC–MS/MS.

Homogeneous Time-Resolved Fluorescence Enzyme Assays. All kinase assays were run at the *K*_m for ATP and quenched within the linearity of the enzyme. All enzyme data described were an average of two determinations, and the Tie-2 data were commonly an average of four determinations. IC₅₀'s for the inhibition of the Tie-2 kinase enzyme for individual compounds were measured using an HTRF assay, utilizing the following procedure: In a 96-well plate (available from Costar Co.) was placed 1 μL of each test and standard compound per well in 100% DMSO having a 25 μM final compound concentration (3-fold, 10-point dilution). To each well was added 20 μL of a reaction mixture formed from Tie-2 (4.0 μL; of a 10 mM stock solution available from Gibco), 0.05% BSA (0.1 μL; from a 10% stock solution available from Sigma-Aldrich Co.), 0.002 mM BLC HER-2 KKK (biotinylated long chain peptide; 0.04 μL; from a 0.002 mM stock solution),

0.01 mM ATP (0.02 μL; commercially available from Sigma-Aldrich Co.), and water (15.84 μL) to bring the total volume to 20 μL/well.

The reaction was initiated in each well by adding 20 μL per well of an enzyme preparation consisting of 50 mM Hepes (1.0 μL; from a 1000 mM stock solution commercially available from Gibco Co.), 0.05% BSA (0.1 μL), 4 mM DTT (0.08 μL; from a 1000 mM stock solution available from Sigma-Aldrich Co.), a 2.4 × 10⁻⁷ M Tie-2 (0.02 μL, from a 4 mM concentration stock), and water (18.8 μL) to dilute the enzyme preparation to a total volume of 20 μL. The plate was incubated for about 90 min at room temperature. After incubation, 160 μL of a filtered detection mixture [prepared from 0.001 mg/mL of SA-APC (0.0765 μL; available as a 2.09 mg/mL stock solution from Gibco), 0.03125 nM Eu-Ab (0.1597 μL; available in a 31.3 nM stock solution from Gibco), and water to bring the total volume to 160 μL (159.73 μL)] was added to each well to stop the reaction therein. The plate was then allowed to equilibrate for about 3 h and read on a Ruby Star fluorescent reader (available from BMG Technologies, Inc.) using a four-parameter fit using activity base to calculate the corresponding IC₅₀'s for the test and standard compounds in each well.

IC₅₀'s for the inhibition of the KDR kinase enzyme for individual compounds were measured using an HTRF assay, utilizing the procedure described above for the Tie-2 kinase enzyme with the following changes: 1 μM gastrin (Biotin long chain EEEEEYGWLDF), 1 μM ATP, 50 pM His-tagged bisphosphorylated KDR kinase domain, 90 min reaction, 30 min after quench equilibrium; buffers, 50 mM HEPES pH 7.5, 50 mM NaCl, 10 mM MgCl₂, 5 mM MnCl₂, 0.05% BSA, 2 mM DTT.

Conditions for All Other Enzyme Assays. Peptide substrate sequences (all substrates at 1 μM unless stated otherwise) were as follows: gastrin, biotin (long chain) EEEEEYGWLDF free acid; HS-1B, biotin (long chain) EQEDEPEGIYGVLF free acid; HER-2, biotin (long chain) GGMEIYFEFMGKKK free acid; ATF2, biotinylated natural protein substrate, kinase dead, N-term Avitag; PLK, biotin (long chain) AGAGRRRSLELHKR free acid; CDK_1, biotin (long chain) VIPINGSRTPRRGQNR free acid; GFAP, biotin (long chain) RRRITSAARRS free acid; poly EY, from Sigma (P7244), poly(Glu, Tyr) sodium salt (4:1). The following peptides/enzyme constructs were used: PDGF–poly EY/GST KD, TrkA–gastrin/GST KD, EphB4–HS-1B/GST KD, Lck–gastrin/GST KD, Lyn–gastrin/GST FL, CSK–HS-1B/GST FL, Fgr–gastrin/GST KD, Fes–gastrin/GST KD, INSR–gastrin/GST KD, cMet–gastrin/GST KD, Jak3–HER-2/GST KD, Jak2–HER-2/GST KD, Jak1–Tyk2 peptide/GST KD, cKit–HER-2/His KD, Itk–HS-1B/GST KD, p38α–ATF2 (100 nM)/His FL, CDK5–CDK_1/(100 nM)/His FL (KD = kinase domain; FL = full length; GST = glutathione-*S*-transferase tagged; His = His tagged). All assays were quenched within the linearity of the enzyme. All assays were run at the *K*_m for ATP. Buffer conditions for all assays are based on the Tie-2 example with minor variations. PDGF was determined by a radioactive filtration assay. MAPH filter plates and 1 Ci/mmol ³³P were used.

Cell-Based Tie-2 Autophosphorylation Assay. The IC₅₀ of the test compounds for inhibition of Tie-2 autophosphorylation was determined using a plate-based immunoassay using the Delfia detection platform. EA.hy926 cells were cultured in a growth medium solution containing DMEM supplemented with 10% FBS serum and penicillin–streptomycin–glutamine. The cells were plated in 24-well tissue culture plates at a final cell density of 2 × 10⁵ cells/well. The cells were incubated for 5 h at 37 °C. Medium was then removed, and the cells were washed twice with 500 μL of PBS at room temperature. A 500-μL portion of F12 nutrient mixture supplemented with 0.5% FBS was then added to each well, and the cells were incubated at 37 °C overnight. Immediately prior to the addition of test compound, medium was replaced with a preparation of 500 μL of DMEM plus 1% BSA.

Anti-hTie2 antibody (100 μg, R & D Systems, Inc., AF313) was diluted with 10 mL of ice-cold PBS to prepare a 10 μg/mL antibody concentration stock. A 96-well microplate (Perkin-Elmer Wallac,

AAAND-0001) was coated with 100 μL of the anti-Tie-2 antibody stock and the plate was stored at 4 °C overnight. The plates were washed three times with 200 μL of PBS 0.1% Tween20, and blocked for 1 h by 5% BSA. The plates were then stored at room temperature for about 1 h.

A 20- μL aliquot of a selected Tie-2 reference compound was placed in a selected well of a 96-well plate, diluted 1:4 with 100% DMSO from an initial concentration of 10 mM to a final concentration of 2.5 mM, and then diluted 1:3 with 100% DMSO for a 10-point dilution to a final concentration of 0.128 μM . Test compounds (10 μL of a 10 mM concentration) were similarly diluted 1:4 with 100% DMSO to obtain a sample concentration of 2.5 mM and then diluted 1:3 for a 10-point dilution to finally obtain a concentration of 0.128 μM for each test compound. DMSO (20 μL) served as a positive control, and 10 μL of the 2.5 mM reference compound served as the negative control. A 2- μL aliquot from each well (test compounds and positive and negative controls) in the 96-well plate was added to designated wells in the 24-well cell culture plate (1:250 dilution). The culture plate was incubated for 2.5 h at 37 °C. Tie-2 autophosphorylation was then stimulated by the addition of angiotensin I. Recombinant human AngI was diluted to a final concentration of 10 $\mu\text{g}/\text{mL}$ in 1% BSA/DMEM and stored on ice. hAngI (5 μL of 10 $\mu\text{g}/\text{mL}$) was added to each well of the 24-well plate containing the EA.hy926 cells. The plate was then shaken at 700 rpm at 37 °C for about 2.5 min. After shaking, the wells were incubated for a further 7.5 min at 37 °C. The medium was removed and 400 μL of ice cold PBS + 300 μM NaVO_4 was added. The wells were kept on ice for at least 5 min and washed one time with ice-cold PBS containing 300 μM NaVO_4 . The cells were lysed with 150 μL of RIPA, containing 300 μM NaVO_4 and a protease inhibitor cocktail (Sigma-Aldrich, P8340). The cells were lysed on ice for 30 min.

Cell lysate (140 μL) was added to the antibody-coated plate and the plate was incubated at 4 °C for 2 h. The lysate was removed and the plate was washed three times each with 400 μL of Delfia wash buffer. The plate was tap-dried with a paper towel. The anti-phosphotyrosine antibody 4G10 (Upstate, 05-321) was diluted with Delfia assay buffer to make a solution of about 1 $\mu\text{g}/\text{mL}$. Diluted antibody (100 μL) was added to the plate and the plate was incubated at room temperature for 1 h. The plate was again washed three times with 400 μL of wash buffer. Eu-N1-labeled anti-mouse antibody (Perkin-Elmer Wallac, AD0124) was diluted with Delfia assay buffer to a final concentration of 0.1 $\mu\text{g}/\text{mL}$. Diluted antibody (100 μL) was added to each well of the plate and the plate was incubated at room temperature for 1 h. The plate was washed three times as described above. Delfia enhancement solution (100 μL , Perkin-Elmer Wallac, 1244-105) was added to each well and the plate was incubated at room temperature for 5 min in the dark. The europium signal was measured with a Victor multilabel counter (Wallac Model 1420). Raw data were analyzed using a fit equation in XLFit. IC₅₀ values were then determined using Grafit software.

Tie-2 Pharmacodynamic Assay. The effect of **61** on Tie-2 phosphorylation was evaluated in the lungs of female CD-1 NU/NU mice ($n=3/\text{group}$). **61** was administered by oral gavage at 10, 30, and 100 mg/kg at the 0 hour time point. Tie-2 phosphorylation was induced by recombinant human Angiotensin-1 (R&D Systems Inc. Minneapolis, MN). 12 μg of Angiotensin-1 was administered i.v. 15 minutes prior to the 3 hour time point. Then the lungs were immediately dissected and snap frozen in liquid nitrogen. Blood samples were taken by cardiac puncture to determine compound concentrations in the plasma.

Individual mouse lungs were homogenized in 0.75 mL of RIPA buffer containing 300 μM NaVO_4 and a protease inhibitor cocktail (Sigma-Aldrich, P8340). The insoluble debris was removed following centrifugation at 4 °C for 15 min at 14 000 rpm. The supernatants were then precleared with 50 μL of protein A/G agarose beads (Sigma) for 1 h at 4 °C. The supernatants were then centrifuged at 3000 rpm for 2 min and the supernatants decanted into a fresh Eppendorf. The protein concentration of each lysate was determined using the colorimetric RC DC system (Bio-Rad,

500-0121) and the concentration adjusted to 10 mg/mL by dilution in complete RIPA lysis buffer.

Tie-2 was immunoprecipitated from 2 mg of total protein overnight at 4 °C by 4 μg anti-murine Tie-2 antibody (R&D, AF762) in the presence of 50 μL of protein A/G beads (Pierce, 20421). The protein A/G beads were recovered by centrifugation and washed four times in RIPA buffer containing 300 μM NaVO_4 and a protease inhibitor cocktail (Sigma-Aldrich, P8340). The beads were resuspended in 50 μL of 2 \times sample buffer and resolved on a 10% polyacrylamide gel under denaturing and reduced conditions. The proteins were then transferred to a nitrocellulose membrane. The membrane was then blocked overnight in blocking buffer (0.25% gelatin in TBST, 20 mM Tris-HCl pH 7.4, 150 mM NaCl, 0.1% Tween 20). The nitrocellulose filter was then probed with anti-phosphotyrosine 4G10 antibody at a concentration of 0.5 $\mu\text{g}/\text{mL}$ in blocking buffer for 2 h at room temperature. The filter was washed three times in blocking buffer and probed with horseradish peroxidase conjugated anti-mouse IgG (Amersham, NA931V, 1:3000 dilution) for 1 h. The filter was washed three times in blocking buffer. Phosphorylated Tie-2 was detected using a chemiluminescent method and quantified using a chemiluminescent imaging system (Bio-Rad). Images were recorded on Kodak scientific imaging film.

The filter was then stripped and the filter was then probed with the anti-murine Tie-2 antibody (R&D, AF762) for 2 h at room temperature. The blot was washed three times in wash buffer and incubated with horseradish peroxidase linked anti-goat Ig (Dako-Cytomation, P0160, 1:3000 dilution) for 1 h at room temperature. The filter was washed three times in blocking buffer. Total Tie-2 was detected using a chemiluminescent method and quantified using a chemiluminescent imaging system (Bio-Rad). Images were recorded on Kodak scientific imaging film.

Pharmacokinetic Studies. Male Sprague–Dawley rats with surgically implanted femoral vein and jugular vein cannulae were obtained from Charles River Laboratories (Boston, MA). Animals were fasted overnight, and the following day compounds were administered either by oral gavage or by intravenous bolus injection ($N = 3$ animals per study). Oral and iv formulations were made 24–48 h prior to dosing, while intravenous formulations were made on the day of dosing. Blood samples were collected over 24 h via jugular cannula into a heparinized tube. Following centrifugation, plasma samples were stored in a freezer to maintain -70 °C until analysis. Lithium-heparinized plasma samples (50 μL) were precipitated with 100% acetonitrile containing the internal standard (IS). The supernatant was transferred into a 96-well plate, and an aliquot of 20 μL was injected onto an LC–MS/MS system. The analytes were separated by a reversed-phase on a C-18 analytical column. The analyte ions were generated by an electrospray ionization (ESI) source and detected by a Sciex API3000 triple quadrupole mass spectrometer operated in the multiple reaction monitoring (MRM) mode. Study sample concentrations were determined from a weighted ($1/x^2$) linear regression of peak area ratios (analyte peak area/IS peak area) versus the theoretical concentrations of the calibration standards. Pharmacokinetic parameters were calculated using a small molecules discovery assay (SMDA) within the computer program Watson (InnaPhase).

Acknowledgment. We thank Julie Belzile and Perry Novak for a large-scale synthesis of **11**, and Jay Larrow for a large-scale synthesis of **151**.

Supporting Information Available: Elemental analysis, HPLC data, and metabolite identification from microsomal incubation of **61**. This material is available free of charge via the Internet at <http://pubs.acs.org>.

References

- Risau, W. Mechanism of angiogenesis. *Nature* **1997**, *386*, 671–674.
- (a) Walsh, D. A.; Haywood, L. Angiogenesis: A therapeutic target in arthritis. *Curr. Opin. Investig. Drugs* **2001**, *2*, 1054–1063. (b) Detmar, M. The role of VEGF and thrombospondin in skin angiogenesis. *Dermatol. Sci.* **2000**, *24*, S78–S84.
- (a) Folkman, J. Anti-angiogenesis: New concept for therapy of solid tumors. *Ann. Surg.* **1972**, *175*, 409–416. (b) Folkman, J. Tumor angiogenesis: Therapeutic implications. *N. Engl. J. Med.* **1971**, *285*, 1182–1186.
- Toyota, E.; Matsunaga, T.; Chilian, W. M. Myocardial angiogenesis. *Mol. Cell. Biochem.* **2004**, *264*, 35–44.
- Folkman, J. Angiogenesis in cancer, vascular, rheumatoid and other disease. *Nat. Med.* **1995**, *1*, 27–31.
- Shawver, L. K.; Lipson, K. E.; Fong, T. A. T.; McMahon, G.; Plowman, G. D.; Strawn, L. M. Receptor tyrosine kinases as targets for inhibition of angiogenesis. *Drug Discovery Today* **1997**, *2*, 50–63.
- Ferrara, N.; Gerber, H.-P.; Lecouter, J. The biology of VEGF and its receptors. *Nature Med.* **2003**, *9*, 669–676.
- (a) Jones, N.; Iljin, K.; Dumont, D. J.; Alitalo, K. Tie receptors: New modulators of angiogenic and lymphangiogenic responses. *Nature Rev. Mol. Cell Biol.* **2001**, *2*, 257–267. (b) Peters, K. G.; Kontos, C. D.; Lin, P. C.; Wong, A. L.; Rao, P.; Huang, L.; Dewhirst, M. W.; Sankar, S. Functional significance of Tie2 signaling in the adult vasculature. *Recent Prog. Horm. Res.* **2004**, *59*, 51–71. (c) Yu, Q. The Dynamic Roles of Angiopoietins in Tumor Angiogenesis. *Future Med.* **2005**, *1*, 475–484.
- Davis, S.; Aldrich, T. H.; Jones, P. F.; Acheson, A.; Compton, D. L.; Jain, V.; Ryan, T. E.; Bruno, J.; Radziejewski, C.; Maisonpierre, P. C.; Yancopoulos, G. D. Isolation of angiopoietin-1, a ligand for the Tie2 receptor, by secretion-trap expression cloning. *Cell* **1996**, *87*, 1161–1169.
- Maisonpierre, P. C.; Suri, C.; Jones, P. F.; Bartunkova, S.; Wiegand, S. J.; Radziejewski, C.; Copton, D.; McClain, J.; Aldrich, T. H.; Papadopoulos, N.; Daly, T. J.; Davis, S.; Sato, T. N.; Yancopoulos, G. D. Angiopoietin-2, a natural antagonist for Tie2 that disrupts in vivo angiogenesis. *Science* **1997**, *277*, 55–60.
- (a) Sato, A.; Iwama, A.; Takakura, N.; Nishio, H.; Yancopoulos, G. D.; Suda, T. Characterization of TEK receptor tyrosine kinase and its ligands, angiopoietins, in human hematopoietic progenitor cells. *Int. Immunol.* **1998**, *10*, 1217–1227. (b) Kim, I.; Kim, J.-H.; Moon, S.-O.; Kwak, H. J.; Kim, N.-G.; Koh, G. Y. Angiopoietin-2 at high concentration can enhance endothelial cell survival through the phosphatidylinositol 3'kinase/Akt signal transduction pathway. *Oncogene* **2000**, *19*, 4549–4552. (c) Teichert-Kuliszewska, K.; Maisonpierre, P. C.; Jones, N.; Campbell, A. I.; Master, Z.; Bendeck, M. P.; Alitalo, K.; Dumont, D. J.; Yancopoulos, G. D.; Stewart, D. J. Biological action of angiopoietin-2 in a fibrin matrix model of angiogenesis is associated with activation of Tie-2. *Cardiovasc. Res.* **2001**, *49*, 659–670. (d) Mochizuki, Y.; Nakamura, T.; Kanetake, H.; Kanda, S. Angiopoietin 2 stimulates migration and tube-like structure formation of murine brain capillary endothelial cells through c-Fes and c-Fyn. *J. Cell. Sci.* **2002**, *115*, 175–183.
- (a) Lin, P.; Polverini, P.; Dewhirst, M.; Shan, S.; Rao, P. S.; Peters, K. Inhibition of tumor angiogenesis using a soluble receptor establishes a role for Tie-2 in pathogenic vascular growth. *J. Clin. Invest.* **1997**, *100*, 2072–2078. (b) Lin, P.; Buxton, J. A.; Acheson, A.; Radziejewski, C.; Maisonpierre, P. C.; Yancopoulos, G. D.; Channon, K. M.; Hale, L. P.; Dewhirst, M. W.; George, S. E.; Peters, K. G. Antiangiogenic gene therapy targeting the endothelium-specific receptor tyrosine kinase Tie-2. *Proc. Natl. Acad. Sci. U.S.A.* **1998**, *95*, 8829–8834. (c) Siemeister, G.; Schirner, M.; Weindel, K.; Reusch, P.; Menrad, A.; Marmé, D.; Martiny-Baron, G. Two independent mechanisms essential for tumor angiogenesis: Inhibition of human melanoma xenograft growth by interfering with either the vascular endothelial growth factor receptor pathway or the Tie-2 pathway. *Cancer Res.* **1999**, *59*, 3185–3191. (d) Melani, C.; Stoppacciaro, A.; Foroni, C.; Felicetti, F.; Caré, A.; Colombo, M. P. Angiopoietin decoy secreted at tumor site impairs tumor growth and metastases by inducing local inflammation and altering neoangiogenesis. *Cancer Immunol. Immunother.* **2004**, *53*, 600–608.
- Popkov, M.; Jendreyko, N.; McGavern, D. B.; Rader, C.; Barbas, C. F., III. Targeting tumor angiogenesis with adenovirus-delivered anti-Tie-2 intrabody. *Cancer Res.* **2005**, *65*, 972–981.
- Oliner, J.; Min, H.; Leal, J.; Yu, D.; Rao, S.; You, E.; Tang, X.; Kim, H.; Meyer, S.; Han, S. J.; Hawkins, N.; Rosenfeld, R.; Davy, E.; Graham, K.; Jacobsen, F.; Stevenson, S.; Ho, J.; Chen, Q.; Hartmann, T.; Michaels, M.; Kelley, M.; Li, L.; Sitney, K.; Martin, F.; Sun, J.-R.; Zhang, N.; Lu, J.; Estrada, J.; Kumar, R.; Coxon, A.; Kaufman, S.; Pretorius, J.; Scully, S.; Cattley, R.; Payton, M.; Coats, S.; Nguyen, L.; Desilva, B.; Ndifor, A.; Hayward, I.; Radinsky, R.; Boone, T.; Kendall, R. Suppression of angiogenesis and tumor growth by selective inhibition of angiopoietin-2. *Cancer Cell* **2004**, *6*, 507–516.
- (a) Fraley, M. E.; Hoffman, W. F.; Arrington, K. L.; Hungate, R. W.; Hartman, G. D.; McFall, R. C.; Coll, K. E.; Rickert, K.; Thomas, K. A.; McGaughey, G. B. Property-based design of KDR kinase inhibitors. *Curr. Med. Chem.* **2004**, *11*, 709–719. (b) Boyer, S. J. Small molecule inhibitors of KDR (VEGFR-2) kinase: An overview of structure activity relationships. *Curr. Top. Med. Chem.* **2002**, *2*, 973–1000.
- (a) Arnold, L. D. Molecular interactions of potent angiogenesis inhibitors bound to Tie-2. In *Pre-Clinical Development, Protein Kinases in Drug Discovery and Development Conference*, Newark, NJ, Oct 15–16, 2001. (b) Bump, N. J.; Arnold, L. D.; Dixon, R. W.; Hoeffken, H. W.; Allen, K.; Bellamacina, C. (BASF) Method of identifying inhibitors of receptor tyrosine kinase Tie-2 for regulation of neovascularization. WO 01072778, 2001.
- Kasperek, J.; Johnson, N. W.; Yuan, C.; Murray, J. H.; Adams, J. L. *Abstracts of Papers*, 229th National Meeting of the American Chemical Society, San Diego, CA, March 13–17, 2005; American Chemical Society: Washington, DC, 2005; MEDI 134.
- Hodous, B. L.; Geuns-Meyer, S. D.; Patel, V. F.; Albrecht, B. K.; Cee, V. J.; Chaffee, S. C.; Johnson, R. E.; Olivieri, P. R.; Tempest, P. A.; Hughes, P.; Caenepeel, S.; Wang, L.; Bready, J.; Coxon, A.; Kendall, R.; Polverino, A.; Emery, M.; Fretland, J.; Hoffman, D.; Gu, Y.; Rose, P.; Zhao, H.; Long, A.; Gallant, P.; Morrison, M.; Bellon, S.; Kim, J. L. The evolution of a highly selective and potent small molecule Tie-2 kinase inhibitor. *J. Med. Chem.* **2007**, *50*, 611–626.
- Shewchuk, L. M.; Hassell, A. M.; Ellis, B.; Holmes, W. D.; Davis, R.; Home, E. L.; Kadwell, S. H.; McKee, D. D.; Moore, J. T. Structure of the Tie2 RTK domain: Self-inhibition by the nucleotide binding loop, activation loop, and C-terminal tail. *Structure* **2000**, *8*, 1105–1113.
- (a) For, a reference comparing DFG-in, and DFG-out, binding, see: Nagar, B.; Bornmann, W. G.; Pellicena, P.; Schindler, T.; Veach, D. R.; Miller, W. T.; Clarkson, B.; Kuriyan, J. Crystal structures of the kinase domain of c-Abl in complex with the small molecule inhibitors PD173955 and imatinib (STI-571). *Cancer Res.* **2002**, *62*, 4236–4243. (b) For, general references on kinase X-ray, structures, see: Cherry, M.; Williams, D. H. Recent kinase and kinase inhibitor X-ray structures: Mechanisms of inhibition and selectivity insights. *Curr. Med. Chem.* **2004**, *11*, 663–673. Fischer, P. M. The design of drug candidate molecules as selective inhibitors of therapeutically relevant protein kinases. *Curr. Med. Chem.* **2004**, *11*, 1563–1583.
- DiMauro, E. F.; Newcomb, J.; Nunes, J. J.; Bemis, J. E.; Boucher, C.; Buchanan, J. L.; Buckner, W. H.; Cee, V. J.; Chai, L.; Deak, H. L.; Epstein, L.; Faust, T.; Gallant, P.; Geuns-Meyer, S. D.; Gore, A.; Gu, Y.; Henkle, B.; Hodous, B. L.; Hsieh, F.; Huang, X.; Kim, J. L.; Lee, J.; Martin, M. W.; Masse, C. E.; McGowan, D. C.; Metz, D.; Mohn, D.; Morgenstern, K. A.; Oliveira, dos Santos, A.; Patel, V. F.; Powers, D.; Rose, P. E.; Schneider, S.; Tomlinson, S. A.; Tudor, Y.-Y.; Turci, S. M.; Welcher, A. A.; White, R. D.; Zhao, H.; Zhu, L.; Zhu, X. Discovery of aminoquinazolines as potent, orally bioavailable inhibitors of Lck: Synthesis, SAR, and in vivo anti-inflammatory activity. *J. Med. Chem.* **2006**, *49*, 5671–5686.
- Sonogashira, K. In *Metal Catalyzed Cross-Coupling Reactions*; Diederich, F., Stang, P. J., Eds.; Wiley-VCH: New York, 1998; Chapter 5.
- Wilhelm, S. M.; Carter, C.; Tang, L. Y.; Wilkie, D.; McNabola, A.; Rong, H.; Chen, C.; Zhang, X.; Vincent, P.; McHugh, M.; Cao, Y.; Shujath, J.; Gawlak, S.; Eveleigh, D.; Rowley, B.; Liu, L.; Adnane, L.; Lynch, M.; Auclair, D.; Taylor, I.; Gedrich, R.; Voznesensky, A.; Riedl, B.; Post, L. E.; Bollag, G.; Trail, P. A. BAY 43-9006 exhibits broad spectrally oral antitumor activity and targets the RAF/MEK/ERK pathway and receptor tyrosine kinases involved in tumor progression and angiogenesis. *Cancer Res.* **2004**, *64*, 7099–7109.
- Recent studies discount the ability of fluorine to serve as a hydrogen-bond acceptor. See (a) Difluorotoluene, a thymine isostere, does not hydrogen bond after all. Wang, X.; Houk, K. N. *Chem. Commun.* **1998**, 2631–2632. (b) Schmidt, K. S.; Sigel, R. K. O.; Filippov, D. V.; van der Marel, G. A.; Lippert, B.; Reedijk, J. Hydrogen bonding between adenine and 2,4-difluorotoluene is definitely not present as shown by concentration-dependent NMR studies. *New J. Chem.* **2000**, *24*, 195–197.
- Kaplan, D. R.; Martin-Zanca, D.; Parada, L. F. Tyrosine phosphorylation and tyrosine kinase activity of the Trk proto-oncogene product induced by NGF. *Nature* **1991**, *350*, 158–161.

- (26) (a) Tronick, S. R.; Popescu, N. C.; Cheah, M. S. C.; Swan, D. C.; Amsbaugh, S. C.; Lengel, C. R.; DiPaolo, J. A.; Robbins, K. C. Isolation and chromosomal localization of the human *fgf* protooncogene, a distinct member of the tyrosine kinase gene family. *Proc. Natl. Acad. Sci. USA* **1985**, *82*, 6595–6598. (b) Thomas, S. M.; Brugge, J. S. Cellular functions regulated by Src family kinases. *Annu. Rev. Cell Dev. Biol.* **1997**, *13*, 513–609.
- (27) For more information, see the Supporting Information.
- (28) Yutilov, Y. M.; Lopatinskaya, K. Y.; Smolyar, N. N.; Korol, I. V. Unexpected result of imidazo[4,5-*b*]pyridine bromination. *Russ. J. Org. Chem.* **2003**, *39*, 280–281.
- (29) Markevitch, D. Y.; Rapta, M.; Hecker, S. J.; Renau, T. E. An efficient synthesis of 5-bromopyridine-2-carbonitrile. *Synth. Commun.* **2003**, *33*, 3285–3289.
- (30) Guo, F.; Sun, W.; Liu, Y.; Schanze, K. Synthesis, photophysics, and optical limiting of platinum(II) 4'-tolylterpyridyl arylacetylide complexes. *Inorg. Chem.* **2005**, *44*, 4055–4065.
- (31) Kato, Y.; Okada, S.; Tomimoto, K.; Mase, T. A facile bromination of hydroxyheteroarenes. *Tetrahedron Lett.* **2001**, *42*, 4849–4851.
- (32) Tan, H.; Semin, D.; Wacker, M.; Cheetham, J. An automated screening assay for determination of aqueous equilibrium solubility enabling SPR study during drug lead optimization. *J. Assoc. Lab. Automat.* **2005**, 364–373.
- (33) Wright, J. D.; Boudinot, F. D.; Ujhelyi, M. R. Measurement and analysis of unbound drug concentrations. *Clin. Pharmacokinet.* **1996**, *30*, 445–462.

JM061112P